

---

Theses and Dissertations

---

Spring 2013

# Development of a Passive Surface Flux Meter to estimate spatially distributed nutrient mass fluxes

Benjamin Richards Carlson  
*University of Iowa*

Copyright 2013 Benjamin Richards Carlson

This thesis is available at Iowa Research Online: <https://ir.uiowa.edu/etd/2452>

---

## Recommended Citation

Carlson, Benjamin Richards. "Development of a Passive Surface Flux Meter to estimate spatially distributed nutrient mass fluxes." MS (Master of Science) thesis, University of Iowa, 2013.  
<https://doi.org/10.17077/etd.id32gton>.

---

Follow this and additional works at: <https://ir.uiowa.edu/etd>



Part of the [Civil and Environmental Engineering Commons](#)

DEVELOPMENT OF A PASSIVE SURFACE FLUX METER TO ESTIMATE  
SPATIALLY DISTRIBUTED NUTRIENT MASS FLUXES

by

Benjamin Richards Carlson

A thesis submitted in partial fulfillment  
of the requirements for the Master of  
Science degree in Civil and Environmental Engineering  
in the Graduate College of  
The University of Iowa

May 2013

Thesis Supervisor: Adjunct Assistant Professor Nandita Basu

Graduate College  
The University of Iowa  
Iowa City, Iowa

CERTIFICATE OF APPROVAL

---

MASTER'S THESIS

---

This is to certify that the Master's thesis of

Benjamin Richards Carlson

has been approved by the Examining Committee  
for the thesis requirement for the Master of Science  
degree in Civil and Environmental Engineering at the May 2013 graduation.

Thesis Committee: \_\_\_\_\_  
Nandita Basu, Thesis Supervisor

\_\_\_\_\_  
Craig L. Just

\_\_\_\_\_  
Jerald L. Schnoor

To those closest to me, Allie, Mom, Dad, Jonathan, Melissa.

Wilderness is not a luxury but a necessity of the human spirit, and as vital to our lives as  
water and good bread.

Edward Abbey  
Desert Solitaire

## ACKNOWLEDGMENTS

I would first like to thank Dr. Nandita Basu for allowing me to work on this project, for her immense patience with me through the learning process, and for guiding me down the right paths when I could not find one. I would like to thank Sam Boland for passing on his knowledge of the PSFM and helping me understand the intricate nature of the methods.

I would like to thank Dr. Rich Valentine for his insight on the spectrophotometric methods of detecting nitrate in brine solutions, Dr. Craig Just for helping me work through my methods, and Dr. Jerry Schnoor for informing me about the history of the research done on Clear Creek.

I would also like to thank all of the people who helped me around the labs, Collin Just for helping with GC methods, Jonathan Durst for all his help and work during the lab manager transition, and Brandon Barquist, and Tim Houser for helping with the flume. I would also like to thank Dr. Caronline Davis for allowing me to use her Nitratax nitrate data, and Sarani Rangarajan for taking pictures of the deployment process. I would also like to thank Steven Sassman from Purdue University for his work on the alcohol tracers and characterization of the sampler.

I would like to thank all of the student workers who helped me throughout my research including Emery Waterhouse, Zexi Liu, Nick Leach, and especially Brett Zimmerman, without the help of these young men I would have been spending many long nights in the lab analyzing data. I would also like to thank all my colleagues in the EES and IIHR programs who supported me during my time here.

I would like to thank my family, Mom you are an amazing strong women who works hard to support her family and put all three of your children through higher education. Dad, even though we live 10 hours apart the phone calls and talks we had really helped keep me motivated. Jonathan, your work through two masters programs

allowed me to see the hard work and dedication it takes to earn a master's degree. Melissa, your bright spirit and attitude inspire me and you bring joy into my heart every time we get together. Finally, I would like to thank the love of my life Allie who supported me through this process, even though we were half a continent apart for most of it. You kept me going through the struggles and pushed me to be a better person.

## ABSTRACT

Due to recent changes in agricultural practices the nutrient load in our waterways has increased causing eutrophication and hypoxia. Many legislative actions have taken place because of this problem, including the Clean Water Act of 1972 (CWA), and many different nutrient reduction plans. The CWA governs that impaired waterways must be monitored to meet total maximum daily loads (TMDL) for each watershed. TMDL's must be assessed using data collected over a period of time so that reduction techniques can be administered. TMDL assessments are usually conducted by the United States Geological Survey (USGS) through many different monitoring programs. The USGS programs include collecting streamflow and nutrient concentration data and using the information to estimate nutrient loads. Generally, grab sampling is the method of choice for concentrations. Grab samples do not accurately assess the total load as generally only 6-8 samples can be collected over a year due to financial and logistical constraints, while concentrations vary within a span of hours and days. Research applications involve the use of automated sensors (e.g., ISCO) that allow for more frequent sampling in order to overcome this issue but are expensive to purchase and maintain. Thus the development of an inexpensive, passive sampler would be of much interest in estimating load. The Passive Surface Flux Meter (PSFM), an integrative sampler that estimates the total solute load over a storm event, is such an alternative. The PSFM is composed of two sorbents one to collect the contaminant of choice and another to determine the flow through the device. Ion-exchange resin was used to collect nitrates, while Granular Activated Carbon dosed with a suite of alcohols were used to determine flow through the sampler. This thesis sets forth the fundamental theories behind the PSFM, and investigates its ability to measure nutrient fluxes in the field. In-situ deployments within Clear Creek watershed in Iowa were conducted using a modification of the PSFM design by Boland (2011). There was a strong linear relationship between the loads estimated by the PSFM, and "true"



load based on USGS stream gage data, and Nitratax sensor data. This implies that the device could be calibrated to work in the field. However, it was determined that the design underestimated the true load in the stream by 29%. This was attributed to the non-linear relationship between the external velocity and the flow through the sampler, which weighted the results towards the high flow events. To overcome this constraint, a new design is proposed in which flow through the sampler varies linearly with the transient head at the inlet. Flume experiments done under different flow depths proved that linearity conditions were satisfied. Using the results from the laboratory experiments recommendations were made for design of an in-situ deployment of the new design.

## TABLE OF CONTENTS

LIST OF TABLES.....	X
LIST OF FIGURES .....	XI
CHAPTER 1: INTRODUCTION.....	1
1.1 Motivation.....	1
1.2 Nutrient Loading Problem.....	2
1.3 Total Maximum Daily Load (TMDL) Estimates.....	3
1.4 Surface Water Monitoring.....	4
1.4.1 Active versus Passive Sampling.....	7
1.5 Passive Sampling.....	7
1.5.1 Time-integrated versus Flow-integrated Sampling.....	11
1.5.2 Background on Existing Designs .....	12
1.6 Objectives .....	14
CHAPTER 2: DEVICE THEORY, CONSTRUCTION, AND FLUME EXPERIMENTS.....	15
2.1 Introduction.....	15
2.2 Principles of the Passive Surface Flux Meter (PSFM).....	15
2.2.1 Estimating flow through the PSFM.....	15
2.2.2 Estimating Ambient Stream Flow .....	17
2.2.3 Estimating Nitrate Mass Flux and Flow-averaged Concentration through the PSFM.....	18
2.2.4 Correlating PSFM Measurement to Flow-averaged Concentration in the Stream.....	19
2.3 Device Assembly and Material Characterization .....	19
2.3.1. Device Assembly.....	19
2.3.2 Characterization of the GAC Layer.....	23
2.3.3 Characterization of the Resin Layer.....	24
2.3.4 Sand Layer.....	27
2.4 Sampler Preparation, Deployment, and Extraction .....	31
2.4.1 Loading of Alcohols to Granular Activated Carbon .....	31
2.4.2 Sampler Packing and Deployment .....	31
2.4.3 Analysis of Nitrate and Alcohol Tracers Post Deployment .....	32
2.5 Data Analysis.....	34
2.5.1 Estimation of Water Flux .....	34
2.5.2 Estimation of Nitrate Flux.....	34
2.5.3 Estimation of Flow Averaged Concentration .....	34
2.6 Summary.....	35
CHAPTER 3: CLEAR CREEK FIELD DEPLOYMENT.....	36
3.1 Introduction.....	36
3.2 Field Site Description .....	36
3.3 PSFM Field Deployment Methods .....	39

3.4 Results.....	42
3.4.1 Flow-averaged Concentration .....	42
3.4.2 Solute (Nitrate) Fluxes .....	48
3.5 Discussion.....	50
3.6 Conclusion.....	51
 CHAPTER 4: ALTERNATE DESIGN OF PASSIVE SURFACE FLUX METER.....	 52
4.1 Introduction.....	52
4.2 Device Theory and Construction .....	52
4.2.1 Device Theory .....	52
4.2.2 Device Construction .....	54
4.3 Laboratory Tests to Evaluate Reservoir PSFM Design.....	54
4.3.1 Design of Flume Experiments.....	54
4.3.2 Sorbent Extraction and Analysis .....	56
4.4 Results and Discussion .....	57
4.4.1 Flow Velocity through the Reservoir PSFM.....	57
4.4.2 Nitrate Load and Flux-averaged Concentration Estimated by Reservoir PSFM .....	59
4.5 Design of Field Experiment.....	60
4.6 Conclusion.....	64
 CHAPTER 5: CONCLUSION .....	 66
5.1 Motivation and Objectives.....	66
5.2 Results of In-situ Field Deployments .....	66
5.3 Results of Reservoir PSFM .....	67
5.4 Implications and Future Work.....	67
 BIBLIOGRAPHY.....	 69

## LIST OF TABLES

Table 1.1	Typical methods for measurement of stream water parameters and relative costs.....	6
Table 2.1	Retardation factor of alcohol to water for tracer alcohols. ....	24
Table 3.1	Deployment Dates with description of events as well as Nitratax flow averaged concentrations for the Oxford and Coralville sites. ....	40
Table 3.2	Flow-averaged concentrations of nitrate from PSFM and Nitratax for Oxford site.....	45
Table 3.3	Flow-averaged concentrations of nitrate from PSFM and Nitratax for Coralville site. ....	47
Table 4.1	Summary of Flume Experiment Parameters.....	56
Table 4.2	Series of 22 events at the Oxford site using parameters from laboratory experiments to calculate total volume collected over the deployment time.....	62
Table 4.3	Omega values for alcohol after deployment. ....	63

## LIST OF FIGURES

Figure 1.1	Number of articles on applications of passive sampling published between 1999 and mid-2009.....	8
Figure 1.2	Main application areas of passive sampling used to monitor the quality of different environmental compartments between 1999 and mid-2009.....	9
Figure 2.1	Schematic of Passive Surface Water Flux Meter.....	20
Figure 2.2	PSFM design modified from design by (Boland, 2011).....	21
Figure 2.3	Front cap of PSFM with PVC spacer and 70x70 mesh.....	22
Figure 2.4	Back cap of PSFM with 400x400 mesh and plumbers putty to keep it affixed to the cap.....	23
Figure 2.5	Calibration curve for Nitrate in KCl.....	25
Figure 2.6	Calibration curve for Nitrate in Water.....	26
Figure 2.7	Extraction efficiency of nitrate from resin using 2 M KCl extraction method.....	27
Figure 2.8	Falling Head Conductivity test setup.....	29
Figure 2.9	Falling Head Hydraulic Conductivity test of 120 g of 2:1 75:250 um sand mixture for high flow deployment. Effective hydraulic conductivity of 0.37 m/d.....	30
Figure 2.10	Falling Head Hydraulic Conductivity test with 20 g of 2:1 75:250 um sand mixture for low flow field deployment. Effective hydraulic conductivity of 4.97 m/d.....	30
Figure 2.11	Falling Head Hydraulic Conductivity test with 120 g of 2:1 250:75 um sand mixture for use with HD-PSFM testing. Effective hydraulic conductivity of 0.26 m/d.....	31
Figure 2.12	Extraction vials for alcohols and nitrate. The vial on the left is filled with Isobutyl Alcohol and alcohol dosed GAC. The vial on the right is filled with 2 M KCl and ion exchange resin.....	33
Figure 3.1	Land cover map of Clear Creek.....	38
Figure 3.2	Water chemistry probe deployment by IIHR. Probes from left to right are pH, conductivity, temperature, and DO (Hydrolab), Nitrate as N (Hach Nitratax), and turbidity sensor (DTS-12 Forest Technology Systems). Picture courtesy of Sarani Rangarajan.....	39

Figure 3.3	Deployment of PSFM at the Oxford site. The sampler is placed on the downstream post with the upstream post acting as a debris shield. Picture courtesy of Sarani Rangarajan.....	41
Figure 3.4	PSFM deployed about 4 inches below the water surface. Picture courtesy of Sarani Rangarajan. ....	41
Figure 3.5	Instantaneous nitrate data, measured by Nitratax, compared with flux-averaged concentration estimated by the PSFM for the Oxford site.....	43
Figure 3.6	Instantaneous nitrate data, measured by Nitratax, compared with flux-averaged concentration estimated by the PSFM for the Coralville site. ....	44
Figure 3.7	PSFM flow averaged concentration plotted versus Nitratax and USGS discharge flow averaged concentrations at the Oxford site. ....	46
Figure 3.8	PSFM flow averaged concentration plotted versus Nitratax and USGS discharge flow averaged concentration at Coralville site. ....	48
Figure 3.9	Nitrate load estimated by PSFM compared with nitrate load estimated from the Nitratax sensor data and discharge data from the Oxford site.....	49
Figure 3.10	Nitrate load estimated by PSFM compared with estimated nitrate load from Nitratax and discharge data from the Coralville site. ....	49
Figure 3.11	Nitrate load estimated by PSFM compared with estimated nitrate load from Nitratax and discharge data for both sites combined.....	50
Figure 4.1	Experimental set up for flume experiments using the Reservoir PSFM. The reservoir is attached to a post to keep it from floating. The sampler was held at a constant depth using a clamp and ring stand. ....	53
Figure 4.2	Average flowrate through the sampler plotted against the head driving the flow. Flowrate was calculated by the volume of water collected in the reservoir following each experiment. ....	58
Figure 4.3	Average flowrate through the sampler plotted against the head driving the flow. Flowrate was estimated using the alcohol tracers.....	58
Figure 4.4	Flow-averaged concentration of nitrate estimated by alcohol tracers versus ambient concentration of nitrate in flume. ....	59
Figure 4.5	Flow-averaged concentration of nitrate estimated by volume collected versus ambient concentration of nitrate in flume. ....	60
Figure 4.6	Hydrograph of USGS Oxford site.....	61

Figure 4.7    Distribution of 22 events during 2011 with a deployment depth  
of 2.5 ft from the streambed.....61

## CHAPTER 1: INTRODUCTION

### 1.1 Motivation

Over the past century and a half the population on Earth has grown exponentially and accompanying the growth there has been an increasing need for resources including food and water (Tilman, 1999). Due to this increasing demand, trends in food production have increased, leading to changes in land cover. The emergent demand has also altered the agricultural practices of farmers. With the new technology of genetically modified crops and advances in the efficiency of fertilizers, farmers are less likely to use crop rotation and more likely to plant the same crop continuously. These changes in agricultural practices have led to increases in erosion (Stone, 1997), contamination with pesticides, herbicides, hormones, and pharmaceuticals (Durhan, et al., 2006; Fuortes, et al., 1997; Soto, et al., 2004; Winchester, et al., 2009), as well as increased amount of nutrient in our waterways (Diaz & Rosenberg, 2008; Kemp, et al., 2009; Osterman, et al., 2009; Rabalais, et al., 2002; Rabalais, et al., 1996; Smith, et al., 1999). The exponential growth of population on Earth has also led to a growing demand for clean water. The increase in concentration of the aforementioned contaminants in our waterways has led to changes in the water treatment process. More expensive treatment processes must be used to remove the contaminants in order create a drinkable product (Feng, et al., 2012).

The land cover changes have also had a large environmental impact including eutrophication and hypoxia. Eutrophication is the process in which excess nutrients are present in a water body. As a consequence of the increase in the limiting nutrients, for growth of aquatic vegetation, overgrowth takes place which leads to decreased amounts of dissolved oxygen in the water body. Low dissolved oxygen levels in water, known as hypoxia, can lead to fish kills. The limiting nutrient for growth in fresh water is phosphorus, while in salt water it is nitrogen. When the nutrient filled waters of the Mississippi river meet the salt water of the Gulf of Mexico the increased amount of nitrogen, in the water leads to a hypoxic zone near the mouth of the river



(Rabalais, et al., 2002). This zone has led to changes in aquatic habitats and affects the livelihood of many of the fisheries along the gulf coast.

### 1.2 Nutrient Loading Problem

In response to these growing environmental problems the state of Iowa has established the Iowa Nutrient Reduction Strategy (INRS). The INRS was compiled by 23 individuals from multiple organizations throughout the state, and was in order to meet statues of the 2008 Gulf Hypoxia Action Plan, which governs that nitrogen and phosphorus loads to the Mississippi River Basin must be reduced by 45%. Each state within the basin must contribute to the reduction. The two main sources of nitrogen being introduced to Iowa water ways, as well as the entire basin, are point and non-point sources. Point sources include discharge into waterways from industry and wastewater treatment plants, while non-point sources include agricultural and urban runoff and drainage from farm fields. Point source can be controlled more easily because nutrient concentrations are monitored daily and must meet the strict regulations of the National Pollutant Discharge Elimination System (NPDES), which are permits issued by the state for discharge limits of industrial and wastewater treatment plants. But it is non-point sources that attribute to a larger percent of the nutrient load in Iowa waters.

The INRS states multiple alternatives to reduce nutrient loading. For nitrogen reduction the INRS suggested the use of three main groups including nitrogen management practices, land use practices, and edge-of-field removal techniques. Nitrogen management practices includes application timing, sidedressing nitrogen after plant emergence, nitrogen source, application rate, and nitrogen inhibitor, adding cover crops to row crop systems, and adding living mulch to row crop systems. Land use options include changing to perennial crops used for energy production (switchgrass), land retirement, conversion to pasture, and moving from corn-soybean or continuous corn to an extended 4-5 year rotation including multiple years of alfalfa. Edge-of-field removal technologies include drainage water management, shallow drainage, reconstructed wetlands, denitrification bioreactors, and vegetated buffers along streams. The INRS found that

no one technique will reduce the nitrogen load enough but a combination of these practices could. In order to determine if the practices presented by the INRS are meeting the required reduction, the phosphorus and nitrate concentrations in Iowa's water way must be assessed.

### 1.3 Total Maximum Daily Load (TMDL) Estimates

The Clean Water Act of 1972 (CWA) was passed as water quality issues became very evident in the late 1960's with fish kills, and burning rivers. The CWA required by law that states must return all water ways to fishable, swimmable, and drinkable status. The CWA has been largely successful by reducing point source pollution from industrial and municipal waste facilities through the implementation of NPDES permits. However, the CWA lacks in the regulations of non-point source pollutants such as those associated with urban and agricultural runoff (Cooter, 2004). Non-point sources are more difficult to monitor because they are not direct effluents from a source. Adequate characterization of a water body requires significant time and resources to properly sample and process water quality data, making it impractical to monitor every stream, river, and lake within a state.

According to the Clean Water Act of 1972, each state, territory or tribe is required to compile a list of impaired waters and establish ambient water quality standards for each water body (33 USC §1313). For all water bodies that do not meet these standards, a Total Maximum Daily Load (TMDL) must be developed and implemented. A load is defined as the mass of a contaminant entering a waterbody over a period of time. The TMDL quantifies the maximum mass of a pollutant that a water body can receive per day and still meet the water quality standards set forth by the state. A TMDL must be created for each pollutant and should represent the sum of allowable loads for the contaminant including background levels, point and non-point sources, and a margin of safety to account for uncertainties. TMDL development takes many years and requires multiple load assessment approaches to determine water quality standards in a particular water body.

TMDL assessments are made watershed by watershed and must encompass not only the surface waters but also groundwater and atmospheric deposition. The work needed to complete a TMDL depends on the size of the watershed and the severity of the contaminant present. Hence, large-scale studies can be more difficult than small-scale studies but are necessary for determining state, regional, and national water quality. Due to the high amount of manpower needed for a TMDL assessment, the United States Geological Survey (USGS) is assigned to collect the data. Since the beginning of the 20<sup>th</sup> century the USGS has established many different programs monitoring stream data, including discharge, gage height, along with other parameters, and are often used to establish water quality criteria.

For monitoring purposes set forth in the CWA, the INRS, and the 2008 Gulf Hypoxia Action Plan, the main interest is the total load of the contaminant that passes through a stream over a specified time period, the TMDL. The load is often of greater interest in smaller streams as they flow into larger receiving bodies and add to the total load of a larger watershed. Total load,  $L_a$ , can be calculated by integrating the product of the stream discharge,  $Q(t)$ , and the stream concentration,  $C_w(t)$ , as a function of the deployment time  $t$ :

$$L_a = \int C_w(t)Q(t)dt \quad (1.1)$$

#### 1.4 Surface Water Monitoring

In order to make TMDL assessments, both streamflow (L/day) and contaminant concentrations (mg/L) must be measured. The true load in a watershed, is the mass of analyte that passes through the watershed over a period of time. A continuous monitoring of the contaminant concentration and the total discharge from the watershed must be recorded in order to make an accurate assessment.

The most commonly used data collection technique for measuring concentrations in stream water is the grab technique which involves going to a sampling location and analyzing the sample either on site or transporting it back to a lab for analysis. Usually samples are collected 6-8 times a year and are limited by the number of field visits possible in a year and the size of the

watershed. Grab sampling is reliable but only captures the concentration in the stream at a single point in time. When trying to calculate contaminant loads for TMDL assessments, a few grab samples over the year are a poor representation of the total load. Due to the fact that the concentration of a contaminant can vary significantly between sampling times, grab sampling is not a good sampling technique for determining load. Also, the time of highest concern is often during large storm events when runoff from fields increases the discharge in the water body; grab sampling does not capture the size or peak concentrations of these events. As a result of these errors in using grab sampling to estimate load the use of more continuous sampling is resorted to, especially in research applications.

The first type of continuous sampling is an autosampler, the most common being the ISCO<sup>®</sup> line of samplers, which have many different options. The sampler pumps water from the stream into a sample bottle contained within the sampler. The sampler can house many sample bottles which can be filled using different techniques. The sampling regimen can be programmed to take individual samples at different times, or a collection of samples using time-integrated or flow-integrated techniques. Flow is measured by a pressure transducer located at the sampler inlet in the stream. Downsides of autosamplers are, cost (Table 1.1), the limited amount of bottles that can be held within the sampler and the requirement for electricity to power the pump, as well as the need for a trained technician to maintain and deploy/collect the samplers.

Another alternative for data collection is an automated sondes such as a Hydrolab<sup>®</sup>, Hach Nitratax<sup>™</sup>, or YSI electrode. Sondes can be deployed directly in the stream and are connected to a power source and a data logger. The sondes use physical or chemical detection methods in order to determine the amount of a given parameter, such as pH, temperature, conductivity, nitrate concentration, or turbidity. An analog signal of the given parameter is taken and converted to a digital signal which is then logged using a data logger. Though these probes have the ability to measure their given parameter continuously, the amount of energy would be substantial and the amount of data collected would be overwhelming to process and store. Downsides to automated sondes are the cost (Table 1.1), which limits the number of site which

they can be deployed. Also, the sondes must be calibrated by the manufacture once a year and must be maintained by a trained technician.

The previously mentioned devices measure concentrations, and in order to estimate loads concentrations have to be multiplied by the corresponding discharge. Discharge is calculated by creating a rating curve. A rating curve is the relationship between stage height and discharge. By knowing the cross-sectional area at the position of the stage monitor the total area of water at a given stage height can be calculated. Then by knowing the velocity of the stream at that given location, discharge can be determined. By plotting stage versus discharge a relationship can be determined for that specific cross-section of the stream.

Stage is determined using either a stilling well or a pressure transducer. In the stilling well, water from the stream enters and leaves through underwater pipes allowing the water surface inside the stilling well to be at the same elevation as that of the stream. Stage is then measured using a float or a pressure, optic, or acoustic sensor. If a stilling well is not feasible a pressure transducer is used. Stage is determined by maintaining a small flow of gas through a tube place near the stream floor. As the stage increases above the tube, more pressure is required to push the gas through the tube. Costs of a pressure transducer can be seen in Table 1.1.

Table 1.1 Typical methods for measurement of stream water parameters and relative costs.

<b>Parameter</b>	<b>Technology</b>	<b>Typical Cost Range (\$)</b>
Stage	Pressure Transducer	3,000 - 5,000
Stage	Bridge-mounted acoustical sensor	1,000 - 3,000
Water Chemistry	ISCO <sup>®</sup> sampler	5,000 - 7,000
pH, conductivity, TSS, temperature	Hydrolab <sup>®</sup> Sonde	15,000 - 20,000
Nitrate	Hach Nitratax <sup>™</sup> Sonde	15,000 - 20,000
TDS, salinity, ORP, DO	YSI electrode probes	10,000 - 15,000

A cheaper alternative to stilling wells or pressure transducers is an acoustical bridge sensor. The acoustical bridge sensor is mounted on bridge crossing and uses ultrasound technology to determine the change in stage, as well as the velocity, of the stream. Downsides to discharge estimates are cost (Table 1.1), the amount of error that might propagate when using the rating curve, and the amount of manpower needed to maintain the sensor (Alewell, et al., 2004).

#### 1.4.1 Active versus Passive Sampling

The previous methods of detection are considered active sampling, which involves the use of energy for the detection of a given parameter. These data collection strategies can be very effective but also very costly (Table 1.1). When trying to characterize an entire watershed it would be beneficial to use a more economical alternative. One such alternative is by using passive sampling. Passive sampling is dependent on the free flow of an analyte from the aqueous phase to a sorbent due to differential chemical or physical potentials between the two phases. Passive samplers are deployed and allowed to collect analyte during the entire deployment time. Since passive samplers take no external energy source and monitor stream conditions continuously they are an attractive alternative (Gorecki & Namies, 2002; Seethapathy, et al., 2008; Vrana, et al., 2005).

#### 1.5 Passive Sampling

Passive sampling was first used in 1853 by impregnating test paper with potassium iodide to measure ground-level ozone (Namieśnik, et al., 2005). Passive sampling is based on the collection of an analyte by a medium as a result of differences in chemical and physical potentials (Gorecki & Namies, 2002). Passive samplers are very effective when measuring contaminant loads and fluxes, especially when the concentrations of the sample may be very low. Due to its ability to decrease both cost and time of analysis, the use of a passive sampling to collect data for all types of environmental samples has had an increasing trend over the past two decades (Figure 1.1) (Vrana, et al., 2005; Zabiegała, et al., 2010).

Passive sampling is versatile and can easily be adapted for many different applications at a minimal cost, and thus it is a very good alternative for large field studies compared to more active/automated sampling techniques (Figure 1.2). Since contaminant load in water ways are the main concern of the CWA and the INRS, instantaneous data is useful but needs to be integrated over time. Since concentrations can change very rapidly, the use of synoptic sampling can lead to errors in the data if it is not measured continuously. Thus, the use of flux-averaged concentrations collected by a passive sampler can give a better estimate of the true concentration over time (Hatfield, et al., 2002). Passive sampling, requires minimal energy and maintenance requirement, and allows for the collection of a continuous sample; one in which a sampler captures all of the analyte that passes through the device over the deployment period.

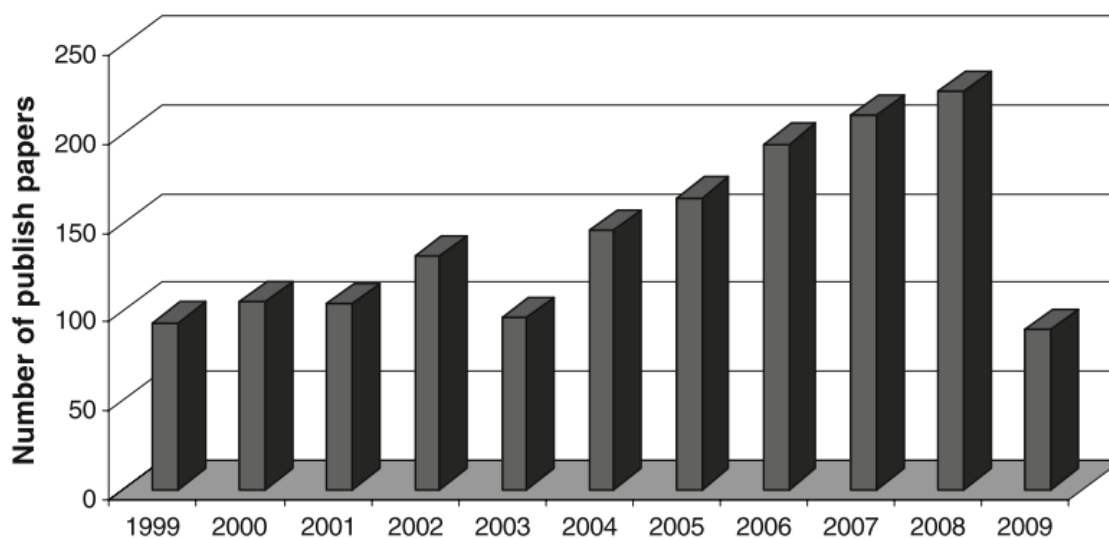


Figure 1.1 Number of articles on applications of passive sampling published between 1999 and mid-2009 (Zabiegała, et al., 2010). Reproduced with permission from Springer Publishing.

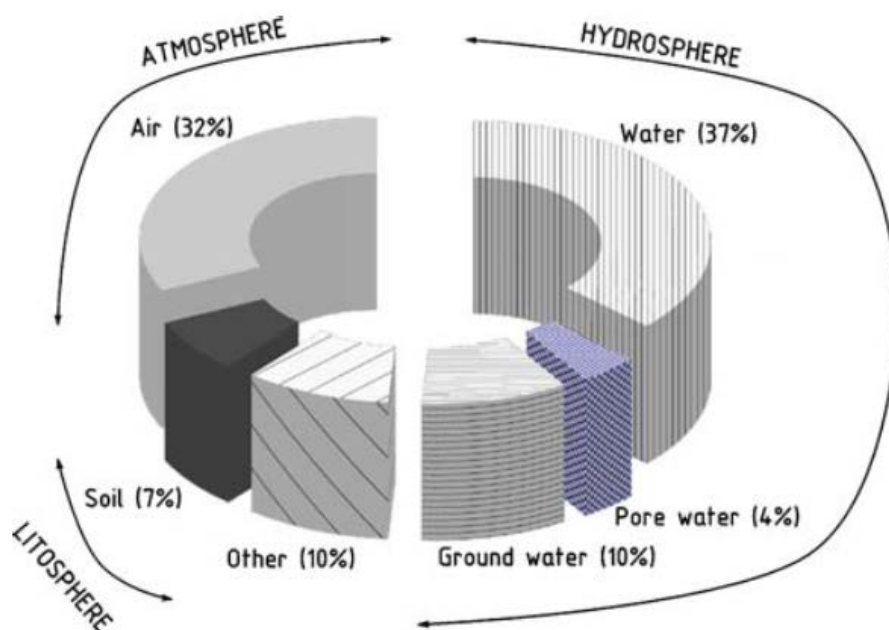


Figure 1.2 Main application areas of passive sampling used to monitor the quality of different environmental compartments between 1999 and mid-2009 (Zabiegała, et al., 2010). Reproduced with permission from Springer Publishing.

The advantage of passive sampling is a minimization in the errors associated with discrete sampling a different time intervals. In discrete sampling, data points are pieced together using different techniques such as linear interpolation, multiple regression, and autoregressive models (Alewell, et al., 2004). In order to reduce errors associated with these techniques, it is necessary to know the frequency of variation in concentration or the autocorrelation time scales. This is also necessary in order to develop a synoptic sampling strategy which is at least twice the frequency of variation. Sample frequencies of this magnitude may not be possible, especially when concentrations may vary over relatively short intervals. Continuous sampling would overcome the fore mentioned problem but would require high cost, high energy, and massive amount of computing power and memory to store the data. Integrative sampling overcomes these



sources of error. Integrated samples remove the need for interpolation, and are extremely useful when trying to make TMDL assessments.

Passive samplers usually have a sorbent phase where the chemical of interest accumulates during the sampler deployment. Partitioning of the chemical from the vapor or aqueous phase to the sorbent phase is typically described by a first-order one compartment mathematical model given:

$$C_s(t) = C_w \left( \frac{k_1}{k_2} \right) (1 - e^{-k_2 t}) \quad (1.2)$$

where  $C_s(t)$  is the concentration of the analyte in the sampler at time ( $t$ ),  $C_w$ , is the concentration of the analyte in the aqueous or vapor phase, and  $k_1$  and  $k_2$ , are the uptake and offload rate coefficients of the sorbent (Vrana, et al., 2005). Passive samplers operate in either an equilibrium or a kinetic accumulation regime. The equilibrium regime, is based on sufficient exposure time to achieve thermodynamic equilibrium between the aqueous/vapor phase and the reference phase. Therefore equation 1.2 reduces to:

$$C_s(t) = C_w \left( \frac{k_1}{k_2} \right) = K_d C_w \quad (1.3)$$

where  $K_d$ , is the phase to water partitioning coefficient. The main requirement for equilibrium based sampling is that the response time required to reach equilibrium is shorter than the fluctuations in  $C_w$  (Mayer, et al., 2003).

For kinetic sampling, conversely, the uptake of the chemical is linearly proportional to the difference in concentration between the aqueous/vapor and receiving phases and the rate of desorption is negligible. This allows equation 1.2 to be reduced to:

$$M_s(t) = C_s R_s t \quad (1.4)$$

where,  $M_s$ , is the mass of the chemical accumulated after time ( $t$ ) and  $R_s$  is a sampling rate based on the product of  $k_1$  and “the volume of water that gives the same chemical activity as the volume of the receiving phase” (Vrana, et al., 2005), providing a volume of water that has had all of the analyte of interest removed. Kinetic samplers are very dependent on the knowledge of the

sampling rate, which can be used to provide a time-averaged concentration in conditions with varying concentrations (Zabiegała, et al., 2010).

### 1.5.1 Time-integrated versus Flow-integrated Sampling

The above mentioned sampling theories have been based on time-integrated sampling, which is the measurement of a solute concentration in a device after an exposure time or the mean of the temporally varying concentrations. The advantages of a flow-integrated sampler over a time-integrated sampler are discussed in full by King & Harmel, 2003. Although, most of the passive samplers used today are time-integrated.

For TMDL assessments load can be calculated by either time-integrated or flow-integrative sampling. The deployment of a time-integrated passive sampler for time  $t$ , measures  $C_t$ , the temporal mean of the concentration by measuring the total mass of contaminant collect by a sorbent over  $t$ . The total load of the deployment,  $L_{et}$ , can be estimated as the product of  $C_t$  and an independent measure of the mean stream flow distribution using a flow recorder:

$$L_{et} = C_t \int Q dt = \int C_w dt \int Q dt \quad (1.5)$$

where  $Q$  and  $C_w$  are often estimated by integrating the 15 minute discharge and concentration of the contaminant over an event. Though  $L_{et}$  is a good estimate of the total load, it is only a reliable approximation under conditions of low temporal variability of the stream concentration.

The use of flow-integrated samplers might give a better estimate. Flow integrated sampling is based on the measurement of both the total flow through the device,  $\forall_d$ , and the total mass of the contaminant sorbed by a media in the device,  $M_d$ . The total flow through the device can be calculated:

$$\forall_d = \int Q_d(t) dt \quad (1.6)$$

where,  $Q_d$ , is the integrated discharge through the device over the deployment time ( $t$ ).

At the same time the sampler collects the contaminant of desire on a sorbent phase in order to calculate the mass flux. The mass flux through the device integrated over the deployment is calculated:

$$M_d = \int Q_d(t)C_w(t)dt \quad (1.7)$$

where,  $C_w(t)$ , is the concentration of the contaminant dissolved in water. The flow-integrated sampler measures  $M_d$ , and  $V_d$  simultaneously using the methods described above and the flux averaged concentration,  $C_f$ , is determined as follows:

$$C_f = \frac{M_d}{V_d} = \frac{\int Q_d(t)C_w(t)dt}{\int Q_d(t)dt} \quad (1.8)$$

The total load of from flow integrated sampling,  $L_{ef}$ , can be calculated:

$$L_{ef} = C_f \int Q dt \quad (1.9)$$

### 1.5.2 Background on Existing Designs

The PFM was originally developed for use in ground water (Hatfield, et al., 2002; Klammler, et al., 2007; Padowski, et al., 2009). The design is comprised of a cylinder filled with a sorbent material that is pre-loaded with alcohol tracers.

The original design for groundwater applications (PFM) were deployed vertically into a monitoring well, so that the flow direction was normal to the orientation of the device. Assuming flow is steady within most groundwater scenarios, consistent relationships between flow through the device and flow in the surrounding media can be derived. Therefore PFMs in groundwater can be used for simultaneous estimation of water and solute fluxes. The method has been successfully verified both in the laboratory and in the field and was applied to investigations of contaminant plume behavior (Annable, et al., 2005; Basu, et al., 2006; Campbell, et al., 2006; Cho, et al., 2007).

The theories behind the PFM were adapted for surface water applications by Klammler, et al., (2007) and then by Padowski, et al., (2009), and re-named as the passive surface water flux meter (PSFM). The main challenge in moving from groundwater to surface water is the order of magnitude increase in the water velocity, and the complexities in open channel flow. In order to overcome this and still be able to measure water flux, specific sampler geometries were deployed. This included a hydrofoil and a cylinder depth sampling apparatus which housed sorbent filled cartridges filled with the alcohol dosed sorbant just as in the PFM. These designs

allowed for a well-defined pressure differential between the inlet and outlet of the cartridges. In addition to the sorbent material of the PFM, the PSFM was packed with two sorbent materials; one to elute the tracers and one to capture contaminants. The sorbent used to capture solutes was an anion exchange resin able to capture dissolved phosphorus. The PSFM was successfully verified both in the laboratory and within an urbanized creek which received treated wastewater (Padowski, et al., 2009). The duration of deployments ranged from 40 to 495 minutes and the environmental settings were close to steady-state. Field applications required the device to be modified under transient flow conditions, which is the focus of Boland (2011) and the current work.

The PSFM designs discussed so far intended to estimate both water fluxes and solute fluxes independently. The biggest difficulty in this approach lies in the complexity of surface water flow fields that leads to flow convergence factor that is difficult to estimate. Interestingly, both the water flux and the solute flux through the sampler are affected by the flow convergence and thus the ratio of the two terms, the flow averaged concentration is arguably unaffected by the geometry. This concentration can then be used in conjunction with an independent estimate of flow to estimate the solute load. This is the essence of the design that was proposed by Boland (2011) and continued in this thesis. Focus in both theses is on nitrate fluxes, since nitrate is one of the most common and easy to measure TMDL candidates.

Boland (2011) developed a three compartment sampler – the first containing an ion exchange resin for sorbing nitrate, the second containing granular activated carbon with presorbed alcohol tracers, while the third was filled with a sand mixture for modulating the hydraulic conductivity. The three materials were characterized in his study, and extraction and measurement techniques for the alcohol tracers and nitrate were developed. A set of flume experiments confirmed the ability of the design to capture the ambient concentrations over certain range of flow velocities. Results from the flume experiment indicated that while the relationship between the external velocity and the velocity through the sampler was linear over certain flow velocity ranges, increasing the range of velocities led to non-linearities.

### 1.6 Objectives

This thesis builds on the research of Boland (2011) to evaluate the PSFM under transient flow in field conditions, and provide alternate designs. Specifically, the study had two objectives:

- (1) Evaluate the ability of the PSFM developed by Boland (2011) to measure nitrate fluxes under transient flow conditions in a natural stream channel.
- (2) Develop an alternate PSFM design based on lessons learned from the field study and test a prototype under laboratory conditions.

In the following chapters these objectives will be presented. In chapter 2 the theories behind the PSFM will be presented as well as all methods for detection of nitrate and alcohol tracers and the corresponding calculations. Laboratory experiments to verify methods are presented along with methods for packing and deploying the sampler for data collection. Chapter 3 presents data from a field experiment in order to meet the first objective. Results will be presented versus actual nitrate flux data. Using results from the field experiment, a new prototype was created using head driven flow through the sampler (objective 2). The theories behind which will be presented in Chapter 4 as well as results from a laboratory experiment and recommendations on field deployment of the new design including sampling depth, duration of deployment, and sampler packing specifications.

## CHAPTER 2: DEVICE THEORY, CONSTRUCTION, AND FLUME EXPERIMENTS

### 2.1 Introduction

In this chapter, the theory of the Passive Surface Flux Meter (PSFM) developed by Klammler, et al., (2007) and then by Padowski, et al., (2009) will be discussed in full, as well as the developments made by Boland (2011). Methods for determining water and mass flux will be discussed, alongside laboratory methods for extraction of contaminants and tracers. Deployment and packing techniques will be discussed, and lastly data analysis will be described.

### 2.2 Principles of the Passive Surface Flux Meter (PSFM)

#### 2.2.1 Estimating flow through the PSFM

The PSFM is comprised of a sorbent layer to collect contaminant mass during a deployment, and a sorbent layer pre-loaded with alcohol tracers to determine the water flux. Estimation of specific discharge through the device by the alcohol tracers is based on three key assumptions: 1) the “resident tracers” are initially uniformly distributed within the device, 2) the tracer transport within the device is homogenous and parallel to the external flow direction, 3) tracer sorption/desorption is linear, reversible, and instantaneous (Hatfield, et al., 2004). The mass flux of any contaminant can be measured by the PSFM as long as 1) the sorbent used can capture the desired contaminant, 2) the total mass of contaminant must be able to be extracted from the sorbent, and 3) the contaminant does not degrade during the deployment time of the device.

The PSFM design by Boland (2011) consists of a tube with conical end fittings which are not filled with sorbent allowing water entering from the tip of the device to diverge to a diameter of the main PSFM tube prior to contacting the sorbent surface (Figure 2.1). The long tubular shape which is aligned parallel to the flow direction ensures flow within the device conforms with the second assumption.

The darcy flux of water through the PSFM,  $q_d$ , is determined by the change in the concentration of a suite of tracer alcohols on Granular Activated Carbon (GAC) (Hatfield, et al., 2004; Cho, et al., 2007).

The water flux is a function of the incremental distance traveled by the tracer,  $dx$ , during the time period  $dt$ , the porosity of the sorbent bed,  $\theta$ , the retardation factor of the tracer to water,  $R_d$ , and the length of the sorbent bed,  $L$ :

$$\frac{q_d}{\theta L} = \frac{dx}{L} \frac{R_d}{dt} \quad (2.1)$$

Assuming, 1)  $dt$ , is the deployment time of the PSFM, 2) purely advective transport of the tracer, and 3) instantaneous sorption/desorption kinetics, then the quantity  $dx/L$  can be represented as the mass of tracer depleted from the PSFM over the deployment time.

$$\frac{dx}{L} = (1 - \omega) \quad (2.2)$$

In which  $\omega$  is the ratio of tracer remaining after deployment and can be calculated:

$$\frac{C}{C_0} = \omega \quad (2.3)$$

where  $C$  is the concentration of alcohol after deployment and  $C_0$  is the initial concentration. The concentration ratio,  $\omega$ , should range between 0.200-0.850 in order to accurately assess the headloss of the device.

Substituting equation 2.2 into equation 2.1 the expression for time averaged specific discharge of water (L/T) through the PSFM is determined:

$$q_d = (1 - \omega) \frac{\theta L R_d}{t} \quad (2.4)$$

Over the deployment period, water passes through the sorbent material and the alcohol tracers wash away at a rate dictated by the tracer's partitioning coefficient ( $K_d$ ) between the sorbed and aqueous phases. The changes in mass of the tracers pre- and post-deployment are used for the estimation of the flowrate through the device ( $Q_d$ ). Concurrently, the sorbent material captures the mass of the desired contaminant that is dissolved in the water, which is used to estimate the mass flux ( $M_d$ ).

$$Q_d = \frac{(1-\omega)A\theta RL}{t} \quad (2.5)$$

$$R = 1 + \frac{K_d \rho_b}{\theta} \quad (2.6)$$

$$M_d = \frac{C_s \rho_b A L}{t} \quad (2.7)$$

where  $C_s$  is the sorbed concentration in the device,  $\rho_b$ , is the bulk density,  $A$  is the cross-sectional area of the sorbent material in the device,  $L$  is the length of the sorbent column, and  $\theta$  is the porosity of the porous media. Porosity is defined as the volume of voids within a porous media divided by the total volume of the media. Bulk density is defined as the mass of porous or particulate media divided by the total volume. The ratio of alcohol tracers remaining,  $\omega$ , is dictated by the retardation coefficient,  $R$ , which describes the velocity of the tracers relative to the velocity of the water passing through the device. The discharge through the PSFM ( $Q_d$ ,  $L^3/T$ ) can thus be determined as a function of the mass fraction of the tracer lost  $\omega$ , and the cross-section area of the sampler,  $A$ .

### 2.2.2 Estimating Ambient Stream Flow

The flow through the PSFM is governed by the external flow field in the stream channel which creates a pressure differential between the inlet and the outlet of the PSFM. Bernoulli's equations can be adapted to estimate the head loss across the PSFM,  $\Delta H$ :

$$\Delta H = \frac{1}{\rho g} (p_1 - p_2) = \frac{1}{2g} (v_2^2 - v_1^2) \quad (2.8)$$

where  $p_1$  and  $p_2$  are the static pressure, and  $v_1$  and  $v_2$  are the local velocities on the PSFM surface at the inlet and outlet, respectively,  $\rho$  is the density of water, and  $g$  is the gravitational acceleration (Hatfield, et al., 2004). The velocity of water at the inlet and outlet can be represented as a function of the undisturbed stream velocity,  $v_o$ , and multiplication factors,  $\chi_1$  and  $\chi_2$ , which is determined based on the shape of the PSFM.

$$\begin{cases} v_1 = \chi_1 v_o \\ v_2 = \chi_2 v_o \end{cases} \quad (2.9)$$

Solving for the velocity of the stream is then possible by substituting equation 2.9 into 2.8 to get:



$$v_o = \sqrt{\frac{2g\Delta H}{\chi_1^2 - \chi_2^2}} \quad (2.10)$$

From Darcy's law, it is known that the darcy flux of water through the device  $q_d$  (L/T) is related to the headloss across the device,  $\Delta H$  (L/T), the length of the device (L), and the saturated hydraulic conductivity of the sorbent  $K$  (L/T):

$$\Delta H = \frac{q_d L}{K} \quad (2.11)$$

Then by substituting equation 2.4 in equation 2.11 the time averaged head difference across the PSFM can be estimated:

$$\Delta H = \frac{L^2 \theta R_d}{K t} (1 - \omega) \quad (2.12)$$

Substituting in equation 2.10, the ambient stream velocity  $v_o$  can be estimated from  $\omega$  and the characteristics of the sorbent:

$$v_o^2 = \frac{2g \left( \frac{L^2 \theta R_d}{K t} (1 - \omega) \right)}{\chi_1^2 - \chi_2^2} \quad (2.13)$$

Within a constant flow field,  $2g/\chi_1^2 - \chi_2^2$  can be assumed to be constant and the pressure head difference between the inlet and the outlet can be represented as the square of the stream velocity:

$$v_o^2 \propto \Delta H \quad (2.14)$$

The caveat in the use of equation 2.13 is that it is not easy to estimate or determine,  $\chi_1$  and  $\chi_2$ , thus leading to errors in the determination of  $v_o$ . While older versions of PSFM have explored the possibilities of estimating  $v_o$  by making assumptions of  $\chi_1$  and  $\chi_2$ , here our focus is primarily to estimate the flux-averaged concentration.

### 2.2.3 Estimating Nitrate Mass Flux and Flow-averaged

#### Concentration through the PSFM

The mass of nitrate (or any solute) captured on the resin is divided by the deployment period to estimate the mass flux through the device adapted from equation 2.7,  $M_d$ .

The flow averaged concentration through the sampler  $C_f^d$  can then be estimated as the ratio between  $M_d$  and  $Q_d$ , as in equation 1.7.

$$C_f^d = \frac{M_d}{Q_d} \quad (2.15)$$

#### 2.2.4 Correlating PSFM Measurement to Flow-averaged Concentration in the Stream

The flow-averaged concentration in the stream ( $C_f^S$ ) can be defined as,

$$C_f^S = \frac{\int Q_s(t)C_s(t)dt}{\int Q_s(t)dt} \quad (2.16)$$

where  $Q_s(t)$ , and  $C_s(t)$ , are the specific discharge of water and the contaminant concentration in the stream respectively. Typically, both  $Q_s$ , and  $C_s$ , are measured at discrete intervals as discussed in Section 1.5 and equation 2.16 is integrated numerically to estimate  $C_f^S$ .

Multiplying the flow-averaged concentration by the total flow volume over a deployment period helps us estimate the solute load over the deployment period. The actual flow-averaged concentration in the stream is different from the estimated  $C_f^d$ , through the PSFM that can be defined as:

$$C_f^d = \frac{\int Q_d(t)C_s(t)dt}{\int Q_d(t)dt} \quad (2.17)$$

The two values  $C_f^d$  and  $C_f^S$  are equal only if there exists a linear relationship between the flow through the device  $Q_d$ , and the streamflow. However, as discussed in equation 2.13, the relationship between the external stream velocity and flow through the device might be non-linear, which might lead to errors in the estimates. A field test under ambient conditions is required to test the relationship between  $C_f^d$  and  $C_f^S$ .

### 2.3 Device Assembly and Material Characterization

#### 2.3.1. Device Assembly

The PSFM is packed with three different materials --- an ion exchange resin in order to capture the nitrate and estimate nitrate flux, Granular Activated Carbon (GAC) dosed with a

suite of alcohols in order to determine water flux, and a sand layer in order to control the hydraulic conductivity of the device. The resin is packed at the upstream end of the sampler so that all of the nutrients are captured before entering the GAC layer, as the GAC layer could also retain some of the nutrients.

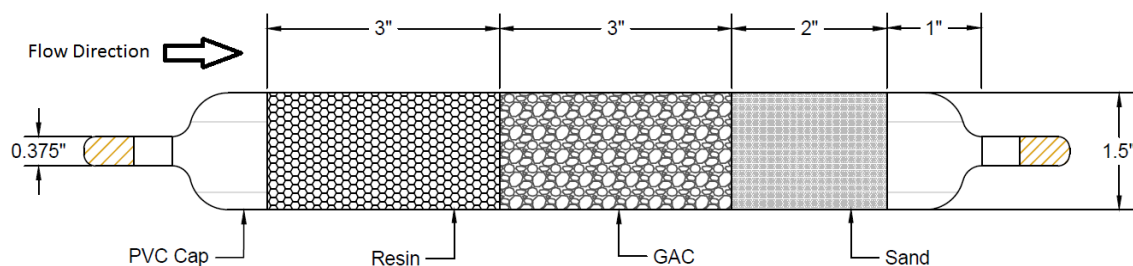


Figure 2.1 Schematic of Passive Surface Water Flux Meter.

The PSFM adapted to a single chamber design from the two chamber design by Boland (2011), due to problems with leaking at the connector causing preferential flow through the device, can be seen in Figure 2.2. The new design is constructed of a 10" section of 1.5" diameter PVC pipe. Male adapters were glued to each end. The inlet cap was created by gluing a 3/8" thread/3/8" brass barb fitting into a 1.5" PVC cap. The front cap of the sampler is affixed with a 1.25" PVC spacer and then a 70x70 mesh in order to keep the sorbents compressed within the sampler (Figure 2.3). The outlet cap was made by gluing a 3/8" thread ball valve/ 3/8" barb into a 1.5" PVC cap. The back of the cap has a mesh size 400x400 in order to keep the sand from leaving the back of the sampler, and was affixed using plumbers putty (Figure 2.4).

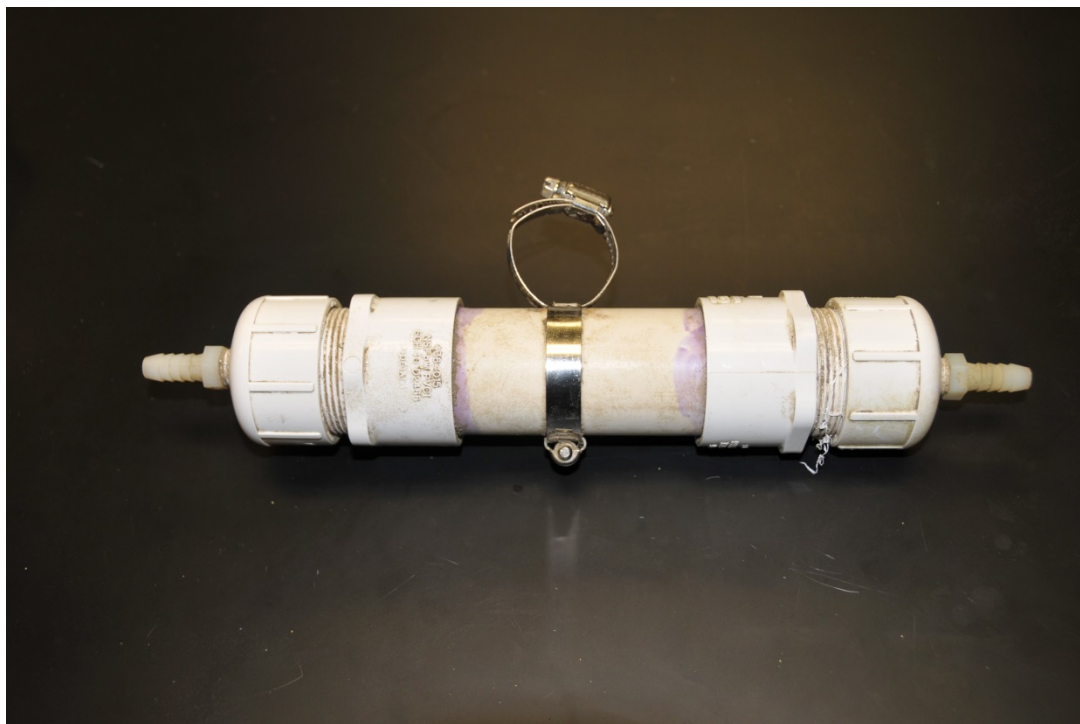


Figure 2.2 PSFM design modified from design by (Boland, 2011).

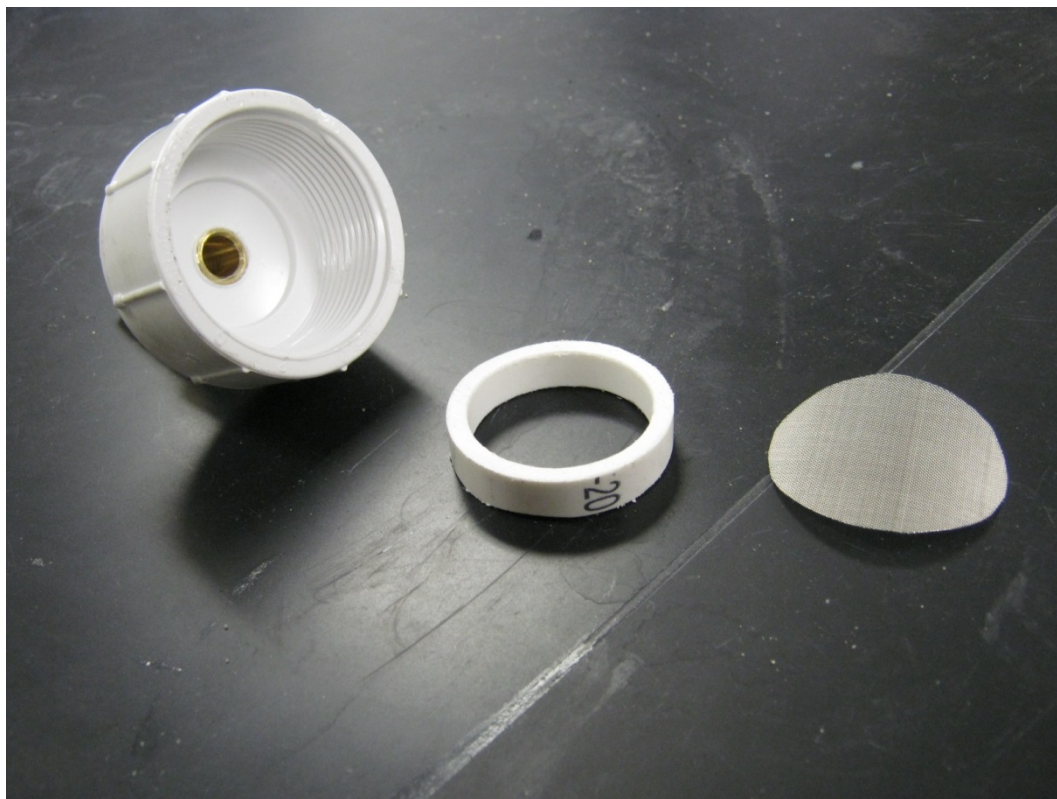


Figure 2.3 Front cap of PSFM with PVC spacer and 70x70 mesh.

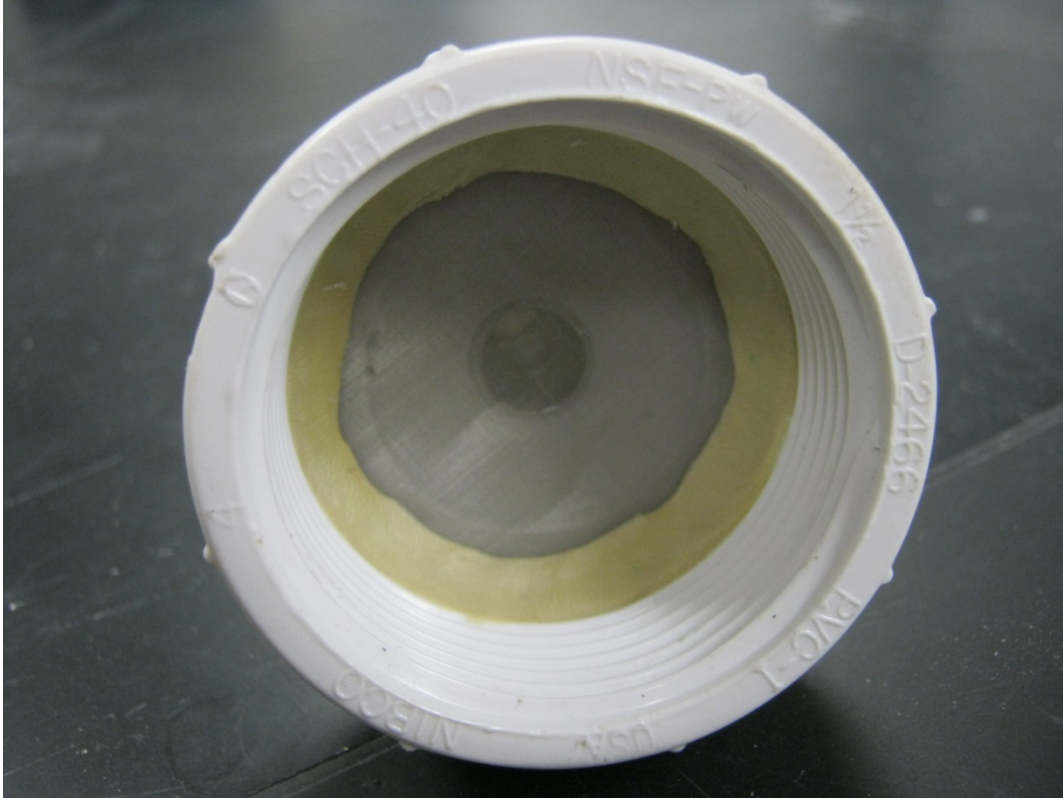


Figure 2.4 Back cap of PSFM with 400x400 mesh and plumbers putty to keep it affixed to the cap.

### 2.3.2 Characterization of the GAC Layer

The GAC is a 12x50 mesh, silver-impregnated granular activated carbon manufactured by Calgon Carbon. The GAC was tested in lab experiments to determine the bulk density, 440 g/L, and the porosity, 0.65 (Boland, 2011). The GAC was preloaded with alcohol tracers, and depletion of the tracers during the deployment was used to estimate the water flux  $Q_d$  through the device, as described in Section 2.2. Four different alcohol tracers were used in order to calculate the water flux, Methanol, Ethanol, 2-Propanol (IPA), and tert-Butyl Alcohol (TBA), while 2,4-dimethyl-3-pentanol (DMP) was used as an internal standard because of its high retardation coefficient,  $R_d$ . The retardation coefficients of the alcohols on the GAC were previously determined by Steve Sassman of Purdue University, and are presented in Table 2.1. Since DMP

has an  $R_d$  an order of magnitude higher than all other alcohols it theoretically should remain the same concentration throughout the deployment period and thus was used as an internal standard.

Table 2.1 Retardation factor of alcohol to water for tracer alcohols.

Tracer	Methanol	Ethanol	Isopropyl Alcohol	Tert-butyl Alcohol	DMP
$R_d$	1.84	6.68	31.5	71.1	1000

### 2.3.3 Characterization of the Resin Layer

An ion exchange resin was used to capture nitrate. The ion exchange resin used was Lewatit MonoPlus MP 500, which is a commercially available product from Lanxess. Lewatit MonoPlus MP 500 is a macro porous anion exchange resin with beads of uniform size designed for demineralization applications. The monodisperse beads have strongly basic amine functional groups which work well to collect positively charged nutrients like nitrate. The mean bead size is  $0.62 \pm 0.05$  mm with a bulk density of 640 g/l (Lanxess, 2006).

In order to determine the extraction efficiency of the contaminant of choice (nitrate) from the resin, a strong ion exchange reaction using 2M KCl to replace the nitrogen was used. Experiments were conducted to estimate the extraction efficiency of the KCl solution to extract nitrate sorbed on the resin. It was previously determined that ~2 g of resin with ~35 mL of extract was an adequate mass/volume ratio for optimal extraction (Boland, 2011). Therefore, 2 g of resin was dosed with ~35 mL of different concentrations of nitrate in water (0, 1, 5, 10, 20 mg/L) and rotated in 40 mL vials for 24 hours, in order to allow for complete sorption of the nitrate on the resin. The supernatant was removed and ~35 mL of the extractant solution (2M KCl) was placed in the vial. The 2M KCl/resin samples were then rotated for 24 hours in order to allow for complete exchange of the potassium ions for the nitrate ions (Cho, et al., 2007).

Following mixing, the samplers were allowed to settle for ~12 hours. The supernatant was then transferred to a glass vial for analysis by spectrophotometry.

Nitrate samples were analyzed using a Varian Cary 50 Bio UV-Vis Spectrophotometer. The spectrophotometer was blanked using the same matrix solution of the samples. The samples were then placed in a 1 cm quartz cuvette and scanned from wavelengths 300 to 200 nm and the absorbance at 260 and 220 nm were recorded. The absorbance at 260 nm is considered the baseline for organics or other interferences in the sample and the absorbance at 220 nm is the nitrate. The baseline absorbance is then subtracted from the nitrate absorbance to give the corrected absorbance (Kaneko, et al., 2012). Calibration curves for nitrate in 2M KCl (Figure 2.5), and water (Figure 2.6) were created using five different concentrations of nitrate (KCl 1, 5, 10, 20, 30 mg/l) (Water 0.1, 1, 5, 10, 20 mg/L).

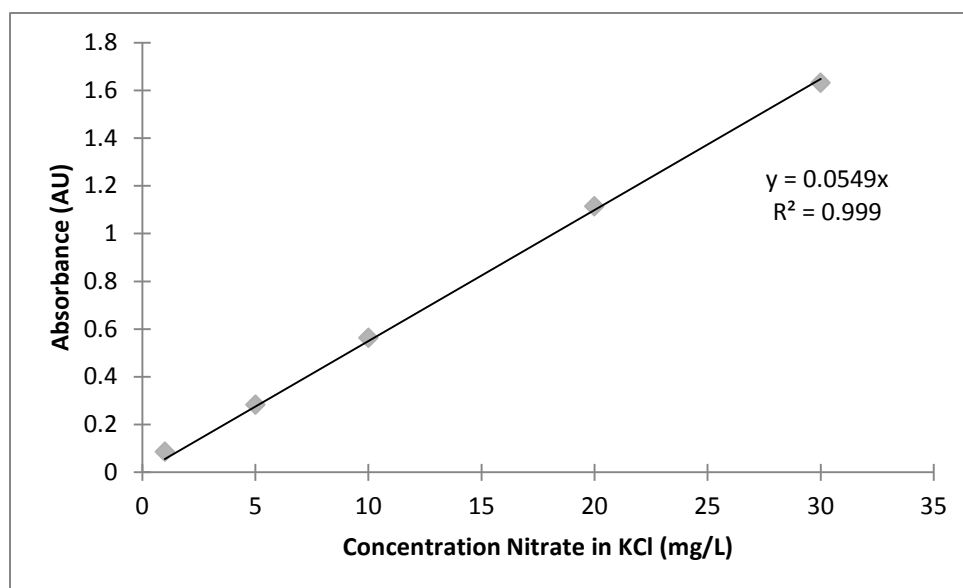


Figure 2.5 Calibration curve for Nitrate in KCl.



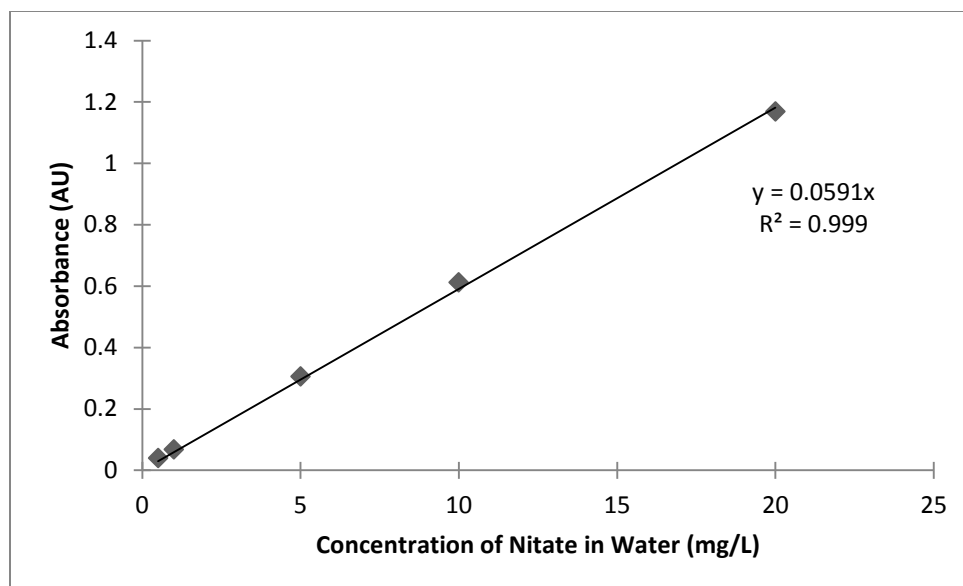


Figure 2.6 Calibration curve for Nitrate in Water.

Using the calibration curve of nitrate in 2M KCl, the concentrations of nitrate (mg/L) in the supernatant KCl solution was determined. This was then multiplied by the volume of 2M KCl used for extraction (~ 35 mL) and then divided by the mass of resin added to the vial (~ 2g) to calculate the total concentration of nitrate on the resin (mg nitrate/g resin) [See equation 2.11].

$$\frac{NO_3^- \left(\frac{mg}{L}\right) * Volume\ of\ KCl\ (L)}{Mass\ of\ Resin\ extracted\ (g)} = NO_3^- \left(\frac{mg}{g}\right) \quad (2.11)$$

Samples of nitrate in water (ambient nitrate) were also run using the same method although the calibration curve in water (Figure 2.6) was used.

The extraction efficiency was determined to be 81% (Figure 2.7) which is the slope of the one to one relationship between extracted nitrate (mg/g) and expected nitrate (mg/g). Expected nitrate was calculated by the concentration of nitrate dosed (1, 5, 10, 20 mg/l nitrate in water) on the resin divided by the total mass of resin used. The non-dosed (0 mg/L) sample was used to determine the amount of nitrate and organics already present on the resin. The mass of interference per mass of resin was then subtracted from the determined mass of nitrate/ mass of

resin and the extraction efficiency was applied in order to calculate the true mass collected on the resin.

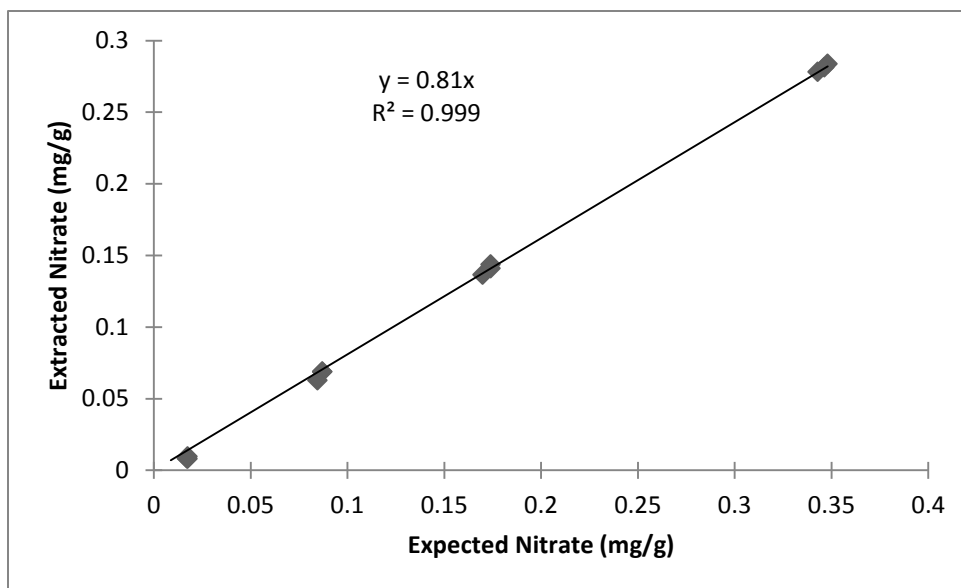


Figure 2.7 Extraction efficiency of nitrate from resin using 2 M KCl extraction method.

#### 2.3.4 Sand Layer

The sand restrictor is used to minimize the variation in  $K$  during the deployment period. control the hydraulic conductivity ( $K$ ) through the sampler. The sand layer is packed at the downstream end so that sediments do not clog the sand, and so that no interactions happen between the contaminants and the sand before entering the sorptive portions of the sampler. If the  $K$  is too low, debris can build up in the front section of the sampler over the deployment time, changing the  $K$  and not accurately determining the external flow or nutrient flux. Also, if flow through the sampler is too high too much of the tracer alcohols will be depleted and flow estimates cannot be sufficiently made. Different combinations of sand particle sizes and lengths of sand layers can be used to increase and decrease the conductivity of the sampler. The sand used was the combination of two U.S. Silica products, F-75 and SIL-CO-SIL 250. Tests were

run in order to determine the best sand ratios and layer thickness. This was done by using Darcy's Law and a falling head column test (Figure 2.8).

$$K = \frac{aL}{At_i} \ln \frac{\Delta h_o}{\Delta h_i} \quad (2.12)$$

Where  $a$ , is the area of the reservoir,  $A$ , is the cross sectional area of the sampler,  $L$ , is the length of the sampler,  $\Delta h_o$ , is the initial head loss at time,  $t = 0$ ,  $\Delta h_i$ , is the head lose at time  $t = i$ .

Three different combinations of fine and medium sized sand grains were used to lead to three different values of effective  $K$  of the resin-GAC-sand column. The flexibility of altering the effective  $K$  of the unit is one of the strengths of the design. For example, drought conditions during 2012 led us to a smaller sand layer thickness to accommodate the low flows. Design 1 for high flow rates, included 120 g of sand with a 2:1 ratio of 75:250 micron sand resulting in a conductivity of 0.37 m/d as shown in Figure 2.9. Design 2 was used in the field to accommodate drought conditions and included 20 g of the same mixture resulting in a  $K$  of 4.97 m/d (Figure 2.10). A third design was used for the head proportional sampler (see Chapter 4), in which the conductivity was lowered using 120 g of a 2:1 ratio of 250:75 micron sand. This combination resulted in a falling head conductivity of 0.26 m/d (Figure 2.11).

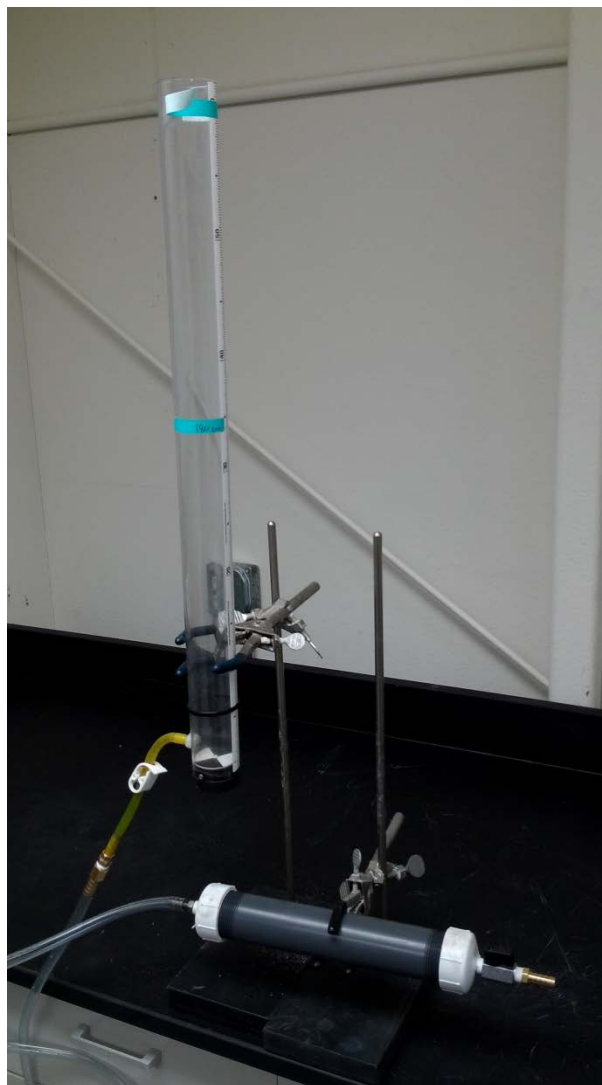


Figure 2.8 Falling Head Conductivity test setup.

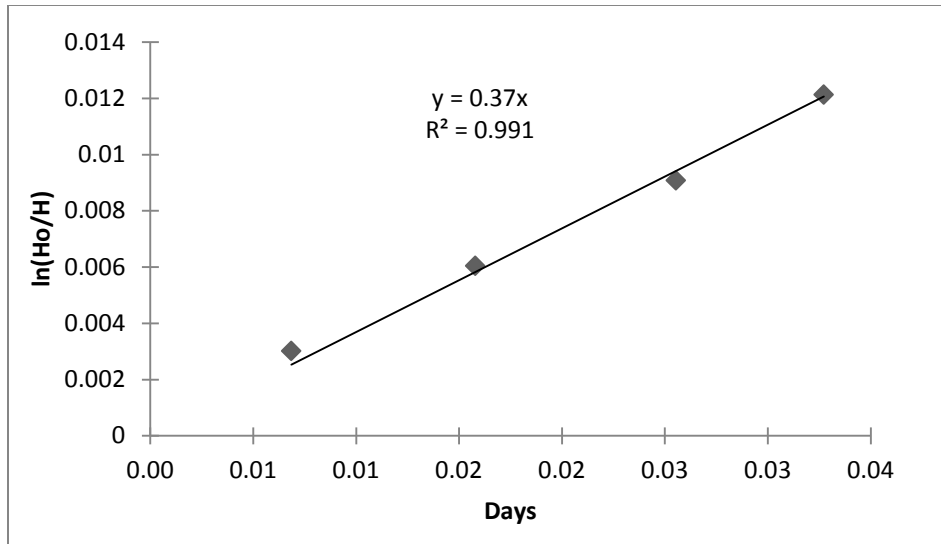


Figure 2.9 Falling Head Hydraulic Conductivity test of 120 g of 2:1 75:250  $\mu\text{m}$  sand mixture for high flow deployment. Effective hydraulic conductivity of 0.37 m/d.

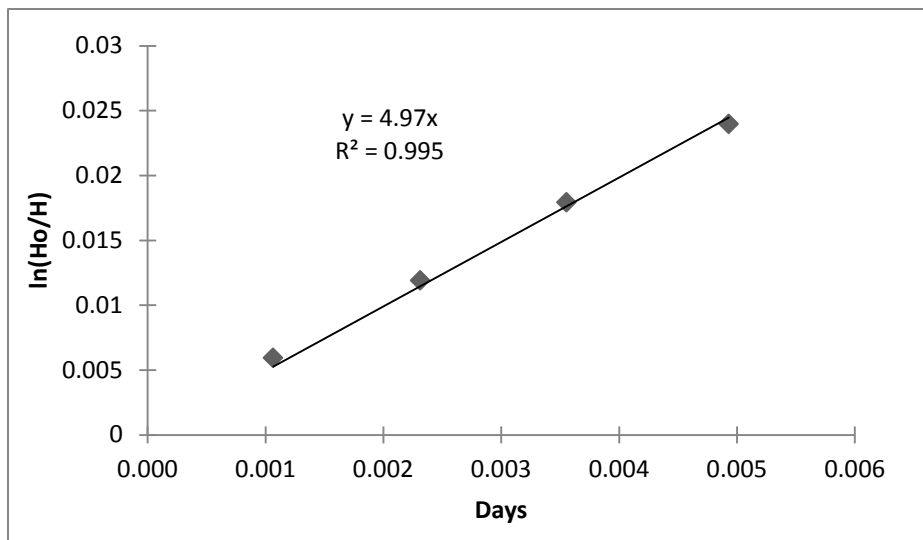


Figure 2.10 Falling Head Hydraulic Conductivity test with 20 g of 2:1 75:250  $\mu\text{m}$  sand mixture for low flow field deployment. Effective hydraulic conductivity of 4.97 m/d.

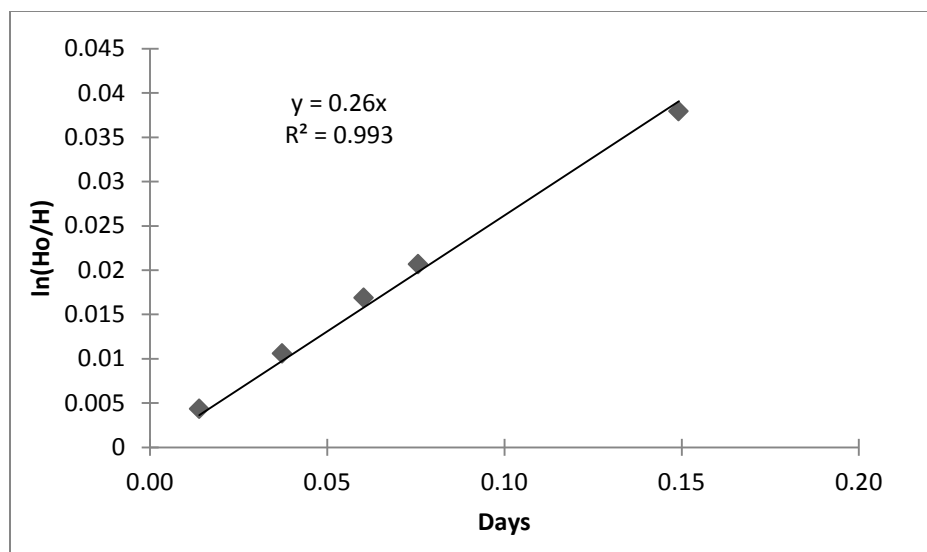


Figure 2.11 Falling Head Hydraulic Conductivity test with 120 g of 2:1 250:75  $\mu\text{m}$  sand mixture for use with HD-PSFM testing. Effective hydraulic conductivity of 0.26 m/d.

## 2.4 Sampler Preparation, Deployment, and Extraction

### 2.4.1 Loading of Alcohols to Granular Activated Carbon

Approximately 200 g of GAC was washed in glass jars using DI water until rinse water was clear. The 5 alcohols were then added into the water, 2 ml each of Methanol, Ethanol, 2-Propanol (IPA), and tert-Butyl Alcohol (TBA), as well as 1 ml of 2,4-dimethyl-3-pentanol (DMP). The solutions was then rotated to allow for sufficient adsorption of the alcohols on the GAC and then stored in a fridge until use in the sampler.

### 2.4.2 Sampler Packing and Deployment

The sampler was packed in the reverse order of flow through the device. First, the sand combination which was to be used for the desired hydraulic conductivity was weighed and mixed. With the ball valve on the back cap closed, the sand was then wet packed into the bottom of the sampler. Next 120 g of the alcohol dosed GAC was weighed and wet packed into the sampler. Next the ion exchange resin (Lewatit MonoPlus MP 500) was packed with the total

mass packed being recorded. Between each layer a piece of glass wool was used to keep the materials from mixing with one another. Once all the layers were packed the front cap was screwed on and water was added to the void space. A cap was then placed on front inlet for transport. Teflon tap was also wrapped around all threading in order to prevent leaking.

Following packing, samplers are stored in a fridge in order to keep any alcohols from releasing due to vaporization. Samplers are also kept on ice during travel. Samplers are deployed in stream at approximately six-tenths from the bottom of the stream stage height in the deepest section of the stream so that samplers remained submerged throughout the deployment time and so erosion of the stream bed did not cover the sampler. Deployment time varies according to the amount and size of storm events that take place during deployment, ideally one deployment should only encompass one storm event but could be deployed for more as long as the alcohol tracers are not completely depleted.

#### 2.4.3 Analysis of Nitrate and Alcohol Tracers Post Deployment

The sorbent and the resin in the PSFM were sampled after retrieval of the sampler from the field site. The anion exchange resin was removed from the sampler, weighed, homogenized and ~2 g of resin was used for extraction using the method described in Section 2.3.2. At least three samples from each sampler were analyzed and averaged for QA/QC.

Pre- and post-deployment samples of the GAC were taken in order to determine  $\omega$ , the mass fraction of alcohol tracer remaining on the GAC. The pre-deployment samples were taken from the excess GAC that was not packed in the PSFM, this sample was exposed to the same conditions as that of the GAC being packed thus should represent the initial concentration of the alcohols that was sorbed to the GAC. After the PSFM had been deployed the GAC layer was completely removed from the sampler. The post-deployment samples well mixed to homogenize the sample and approximately 1.5 g of GAC was placed in a 40 ml glass vial filled with 35 ml of Isobutyl alcohol (Figure 2.12). The tracer alcohols have a higher affinity for other alcohols than for water thus elute from the GAC when mixed. Samples were rotated for 24 hours before being

refrigerated. The supernatants were then transferred to 2 ml GC vials in order to be analyzed by GC-FID.



Figure 2.12 Extraction vials for alcohols and nitrate. The vial on the left is filled with Isobutyl Alcohol and alcohol dosed GAC. The vial on the right is filled with 2 M KCl and ion exchange resin.

Samples were analyzed using an Agilent-6890N GC-FID with a DB-624 column (30 m length, inside diameter of 0.320 mm, film thickness 1.8  $\mu\text{m}$ ). The GC-FID method is as follows. The injection volume was 1  $\mu\text{l}$ . The starting temperature was 80° C for 2.9 minutes followed by a 20° C/min ramp to 250° C and sustained there for 2 minutes. The column pressure was set at 11.9 psi, with an injection split ratio of 30:1. This resulted in a total flow rate of 61.0 ml/min. The detector temperature was 280° C with an air flow of 450 ml/min, an H<sub>2</sub> flow of 40.0 ml/min, with a nitrogen carrier gas as the make-up with a flow of 20 ml/min. Calibration curves,  $R^2 > 0.995$



using 6 different concentrations, 50, 100, 200, 500, 1000, and 2000 mg/L, for each alcohol were created, the slope was used to determine the concentration of alcohol before and after deployment. For statistical analysis samples were taken in at least triplicate and averaged.

## 2.5 Data Analysis

### 2.5.1 Estimation of Water Flux

Measured concentrations of the alcohols pre- and post- deployment were normalized using the concentration of DMP, and replicates were averaged. Then using equation 2.9,  $\omega$ , was determined for each alcohol. The  $\omega$  value was then used in equation 2.16 the time-averaged head loss across the sampler,  $\Delta H$ , is determined for each alcohol. Using the headloss through the device  $\Delta H$ , the flowrate through the device,  $Q_d$  was calculated using equation 2.5. The water flux estimates of the alcohols with  $\omega$  ranging from 0.200 to 0.850 were then averaged to determine the water flux during the deployment.

### 2.5.2 Estimation of Nitrate Flux

Absorbances of the extractant 2M KCl solutions were measured using a Varian Cary 50 Bio UV-Vis spectrophotometer, and converted to concentrations of nitrate using the appropriate calibration curve. Concentrations were then used in equation 2.20 to calculate the total mass of nitrate per mass of resin. The data was corrected by subtracting the interferences from the mass collected and multiplying by the extraction efficiency. Replicates of each deployment were then averaged and the standard deviation was determined. The average and standard deviation were then multiplied by the total mass of resin extracted from the sampler to give the total mass of nitrate collected over the deployment period. This was divided by the deployment period to estimate the nitrate flux  $M_d$ , from equation 1.7.

### 2.5.3 Estimation of Flow Averaged Concentration

The mass flux estimated in Section 2.5.2 was divided by the water flux estimated in Section 2.5.1 to estimate the flow averaged concentration.

## 2.6 Summary

Laboratory experiments were completed in order to determine the proper detection to determine nitrate fluxes using the PSFM. The mass of nitrate collected on the ion-exchange resin was extracted using 2M KCl solution and analyzed using a spectrophotometer. Calibration curves for nitrate in 2M KCl and water were created, and the extraction efficiency was determined to be 81%. Hydraulic conductivity tests were completed in order to determine which combination of sand particles led to adequate flow through the device depending on the flow conditions. For high flow conditions 120 g of 2:1 75:250  $\mu\text{m}$  sand was used resulting in a hydraulic conductivity of 0.37 m/d was used. For low flow conditions 20 g of 2:1 75:250  $\mu\text{m}$  sand was used resulting in hydraulic conductivity of 4.97 m/d. For use with the alternative Reservoir design a sand combination of 120 g of 2:1 250:75  $\mu\text{m}$  sand was used resulting in a hydraulic conductivity of 0.26 m/d. Extraction of the alcohols from the GAC were completed following methods set forth by previous work by Hatfield, Padowski, Basu, Sassman, and Boland.

## CHAPTER 3: CLEAR CREEK FIELD DEPLOYMENT

### 3.1 Introduction

A field deployment experiment was conducted to demonstrate the ability of the PSFM to measure water and solute (nitrate) fluxes under transient flow conditions. This was a natural progression from the flume experiments done by Boland (2011) in which the PSFM was observed to perform adequately under laboratory conditions. The field study was conducted between June and November of 2012 in the Clear Creek Watershed in Iowa. The deployment locations were selected based on the following criteria: 1) accessibility of site and 2) co-located USGS stream gages and IIHR water quality monitoring stations. The second criteria was used to ensure that the solute fluxes measured using PSFM could be validated with independent measurements.

### 3.2 Field Site Description

Clear Creek, a HUC-10 watershed located west of Iowa City, Iowa, has been well studied by researchers at the University of Iowa (Dean, 2011; Loperfido, 2009; Papanicolaou, et al., 2008; Putney, 2010; Rayburn, 2006). Clear Creek drains into the Iowa River. It covers a total land area of 267 square kilometers (Loperfido, 2009). The watershed is comprised of approximately 85% agricultural land, 8% forest cover, 6% roads or urban cover, with the remainder being water or barren land (Figure 3.1) (Loperfido, 2009).

There are two USGS sites located within the watershed one at Oxford (Lat 41°43'06", Long 91°44'24"), which has a drainage area of 151.2 square kilometers, and another at Coralville (Lat 41°40'36", Long 91°35'55") which has a drainage area of 254.1 square kilometers (Figure 3.1). The USGS sites have sensors that monitor gage height at 15-minute intervals. There are also two IIHR Water Quality monitoring stations co-located with the USGS sites, and maintained by Dr. Caroline Davis of The University of Iowa, as a part of the IIHR Nutrient Monitoring study.

The water quality monitoring stations are equipped with sensors Hach Nitratax sc plus 5 mm sensors for nitrate, water chemistry and turbidity that measure these parameters at 15-minute intervals. The Nitratax is connected to a Hach sc200 controller and data was logged by a Campbell Scientific CR1000 datalogger. Since the sensors need a power source in order to collect and store data two 12V marine batteries are used and charged using two 20W solar panels. The electronic equipment is stored at the top of the creek bank. Cords connecting the sensors to the power source and data logger were run down the bank inside 1.5" PVC pipes in order to keep them out of the elements and sensors were deployed in stream inside 4" PVC pipe (Figure 3.2). The sensors were calibrated once a year at the manufacturer, and checked periodically in nitrate standard solutions if problems were observed with the sensor operation. The data was downloaded manually every 1-2 weeks. As a consequence of technical difficulties like battery power outage, or the sensor coming out of the water due to low flow conditions there were times with gaps in the data.

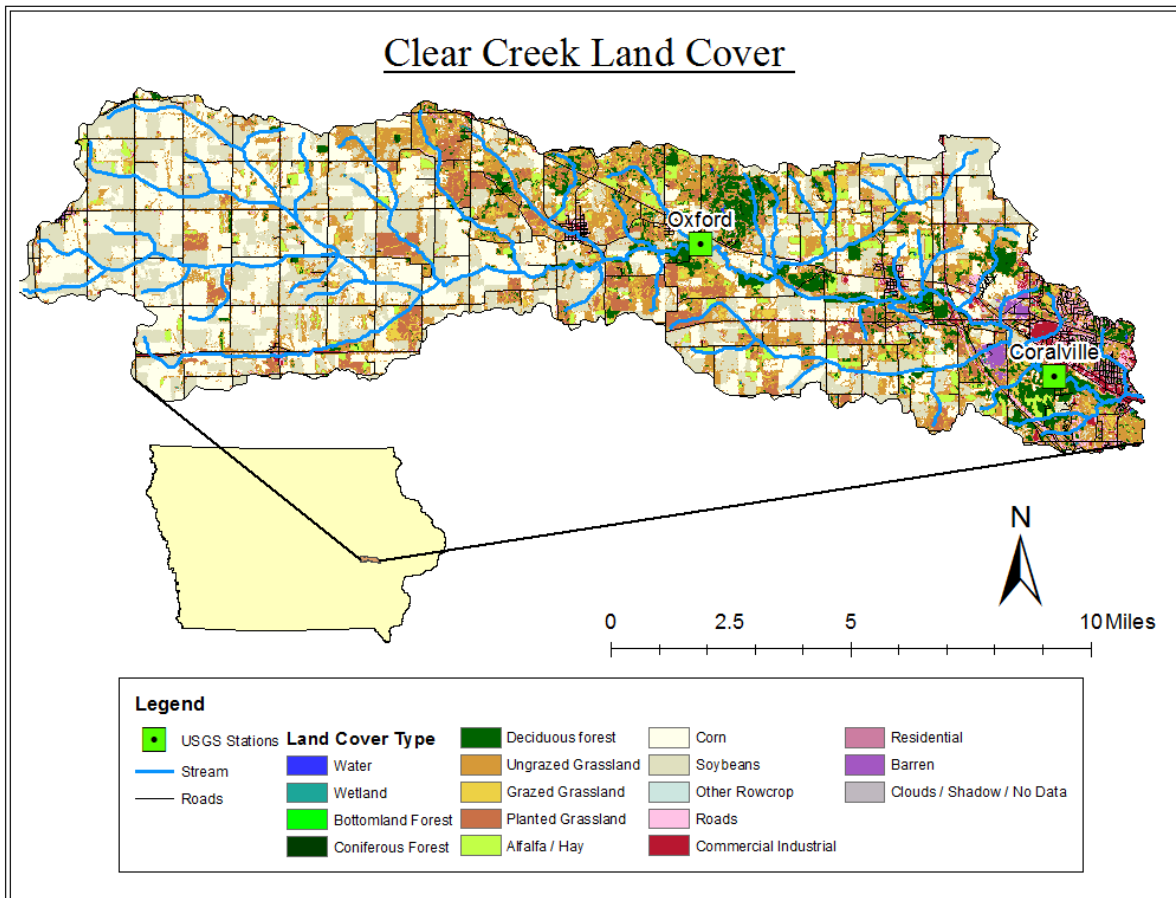


Figure 3.1 Land cover map of Clear Creek.



Figure 3.2 Water chemistry probe deployment by IIHR. Probes from left to right are pH, conductivity, temperature, and DO (Hydrolab), Nitrate as N (Hach Nitratax), and turbidity sensor (DTS-12 Forest Technology Systems). Picture courtesy of Sarani Rangarajan.

### 3.3 PSFM Field Deployment Methods

The PSFMs were deployed almost every week (Table 3.1) at both the Coralville and the Oxford site. Since 2012 was a drought year a lot of deployments did not lead to measurable water flow and solute flux data. The samplers were packed in the laboratory prior to traveling to the field site. At the site, the PSFMs were affixed to a t-post, using hose clamps. Two t-posts were driven into the creek bed, the first post was used as a debris-block so that large debris such as leaves or twigs did not block flow into the PSFM, which was positioned on the second post

(Figure 3.3). The samplers were placed in the stream parallel to the flow direction with the resin at the upstream end (Figure 3.4). Samplers were placed at approximately 6/10 of the depth from the bottom so that the sampler would be submerged throughout the deployment period. After approximately one week of deployment the PSFMs were collected and brought back to the lab for analysis. Samplers were kept in a cooler during travel time to minimize volatile losses of the alcohol tracers.

Table 3.1 Deployment Dates with description of events as well as Nitratax flow averaged concentrations for the Oxford and Coralville sites. Events with no data are due to no data from the Nitratax due to low flow events or power outages. <sup>1</sup> Drought conditions caused flow averaged concentrations to decrease between deployments.

Deployment Date	Retrieval Date	Nitratax C <sub>f</sub> Oxford	Nitratax C <sub>f</sub> Coralville	Conditions
6/8/2012	6/15/2012	34.10	N/A	Small Event
6/20/2012	6/27/2012	28.18	19.22	No Event
6/27/2012	7/5/2012	20.45	12.32	No Event
7/25/2012	8/1/2012	3.26	2.66	No Event <sup>1</sup>
8/1/2012	8/8/2012	N/A	3.86	No Event
8/14/2012	8/22/2012	4.58	3.16	No Event
8/22/2012	8/28/2012	4.77	2.34	No Event
8/28/2012	9/5/2012	5.73	2.83	Small Event
9/5/2012	9/12/2012	6.68	3.99	Small Event
9/12/2012	9/19/2012	7.99	3.50	Medium Event
9/19/2012	9/26/2012	10.75	2.05	Large Event at Oxford
9/26/2012	10/3/2012	6.19	3.52	Small Event
10/3/2012	10/10/2012	1.45	2.29	No Event
10/10/2012	10/17/2012	4.35	3.56	No Event
10/17/2012	10/24/2012	3.22	N/A	Small Event
10/24/2012	10/31/2012	4.29	4.25	No Event
10/31/2012	11/7/2012	4.97	6.97	Small Event



Figure 3.3 Deployment of PSFM at the Oxford site. The sampler is placed on the downstream post with the upstream post acting as a debris shield. Picture courtesy of Sarani Rangarajan.



Figure 3.4 PSFM deployed about 4 inches below the water surface. Picture courtesy of Sarani Rangarajan.



Once samplers had been brought back to the lab the resin and activated carbon were removed from the samplers for their separate extraction methods following the methods in subsection 2.4.3 and data was analyzed using the methods from Section 2.5.

### 3.4 Results

#### 3.4.1 Flow-averaged Concentration

The PSFM measures a flow-weighted concentration averaged over the duration of the deployment,  $C_f$ , according to methods stated in Chapter 2. The  $C_f$  was compared with the instantaneous concentrations measured by the Nitratax sensors for the Oxford site in Figure 3.5 and the Coralville site in Figure 3.6. In the mean, the PSFM results underestimated the instantaneous concentrations.

The flow-averaged concentrations from PSFM were also compared with flow-averaged concentrations estimated using the Nitratax sensor. Nitrate concentrations measured by the sensor were multiplied with the USGS estimated discharge to estimate nitrate loads on a 15-minute timescale. The load was integrated over the duration of the event, and divided by the total discharge during the event to estimate the flow-averaged  $C_f$ . Similar to the observation from Figures 3.7 and 3.8, the PSFM resulted in a lower  $C_f$  than those estimated from the Nitratax sensor (Table 3.2 and 3.3). It can be seen that at the higher flow events the PSFM is overestimating the Nitratax  $C_f$  while at the lower flow events it is underestimating.

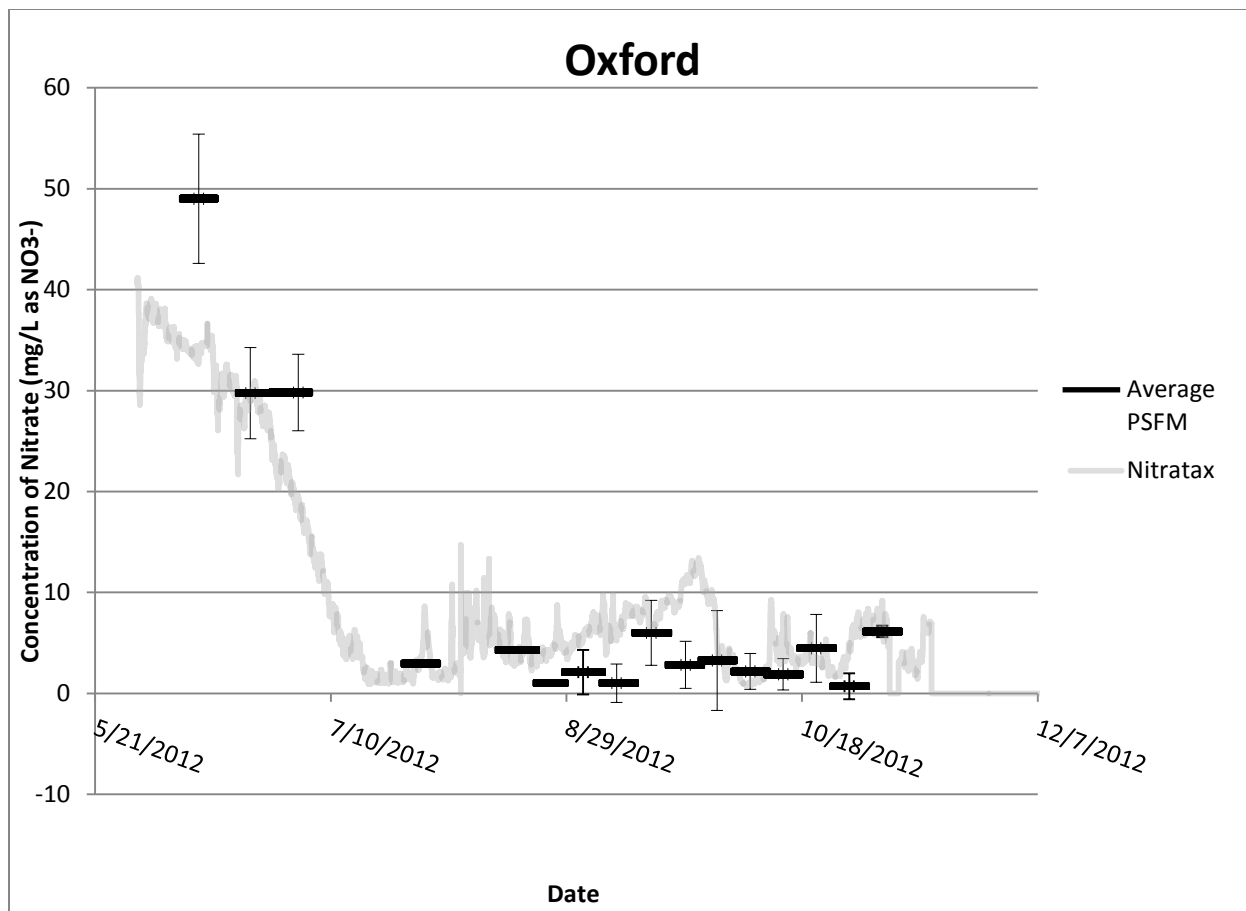


Figure 3.5 Instantaneous nitrate data, measured by Nitratax, compared with flux-averaged concentration estimated by the PSFM for the Oxford site.

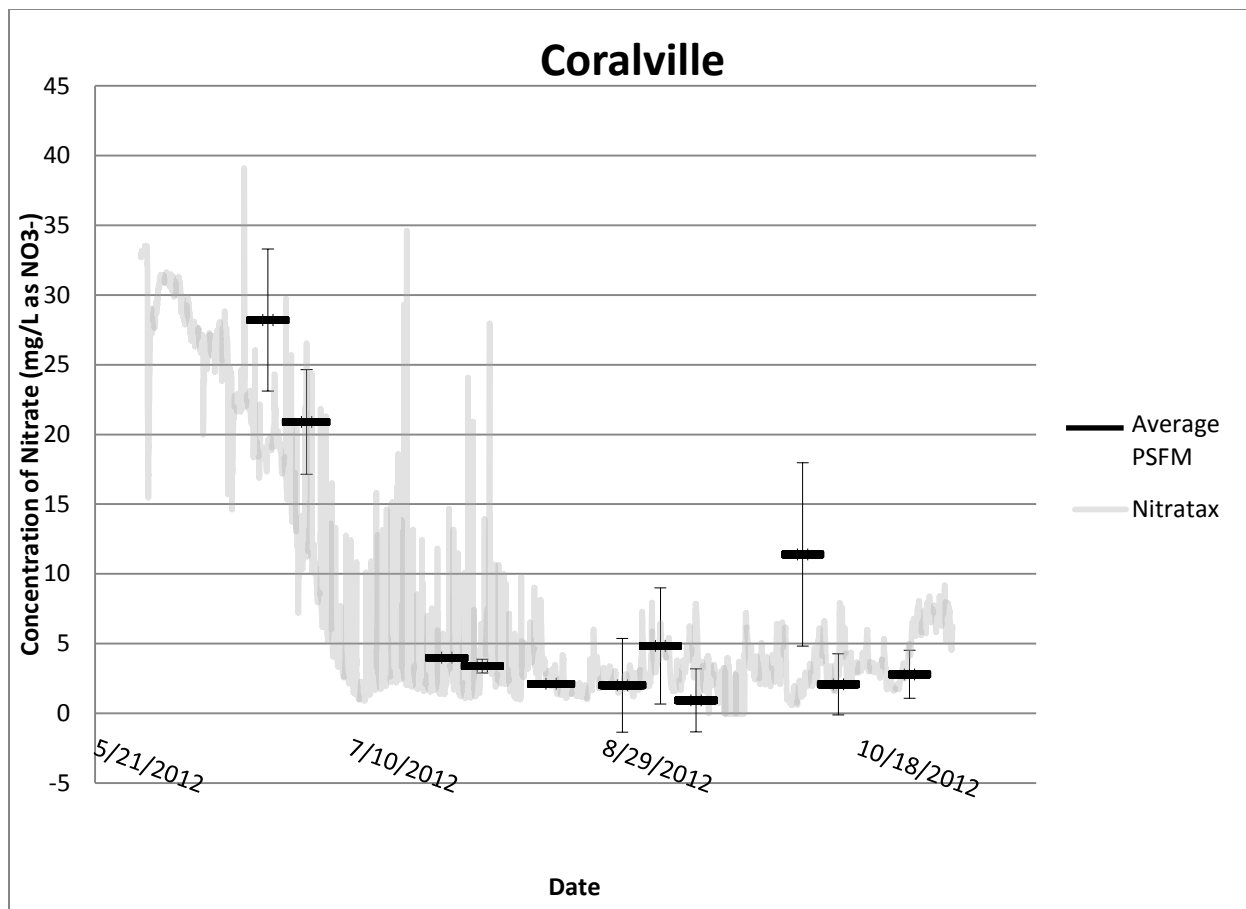


Figure 3.6 Instantaneous nitrate data, measured by Nitratax, compared with flux-averaged concentration estimated by the PSFM for the Coralville site.

Table 3.2 Flow-averaged concentrations of nitrate from PSFM and Nitratax for Oxford site.

Deployment Date	Collection Date	PSFM Mean Cf	PSFM Standard Deviation	Nitratax Cf
6/8/2012	6/15/2012	49.01	6.11	34.1
6/20/2012	6/27/2012	29.74	4.52	28.18
6/27/2012	7/5/2012	29.81	3.79	20.45
7/25/2012	8/1/2012	2.97	0.17	3.26
8/14/2012	8/22/2012	4.29	0.01	4.58
8/22/2012	8/28/2012	1.01	0.17	4.77
8/28/2012	9/5/2012	2.11	2.2	5.73
9/5/2012	9/12/2012	1.02	1.9	6.68
9/12/2012	9/19/2012	6.01	3.21	7.99
9/19/2012	9/26/2012	2.84	2.33	10.75
9/26/2012	10/3/2012	3.26	4.94	6.19
10/3/2012	10/10/2012	2.18	1.77	1.45
10/10/2012	10/17/2012	1.89	1.54	4.35
10/17/2012	10/24/2012	4.46	3.36	3.22
10/24/2012	10/31/2012	0.7	1.28	4.29
10/31/2012	11/7/2012	6.14	0.58	4.97

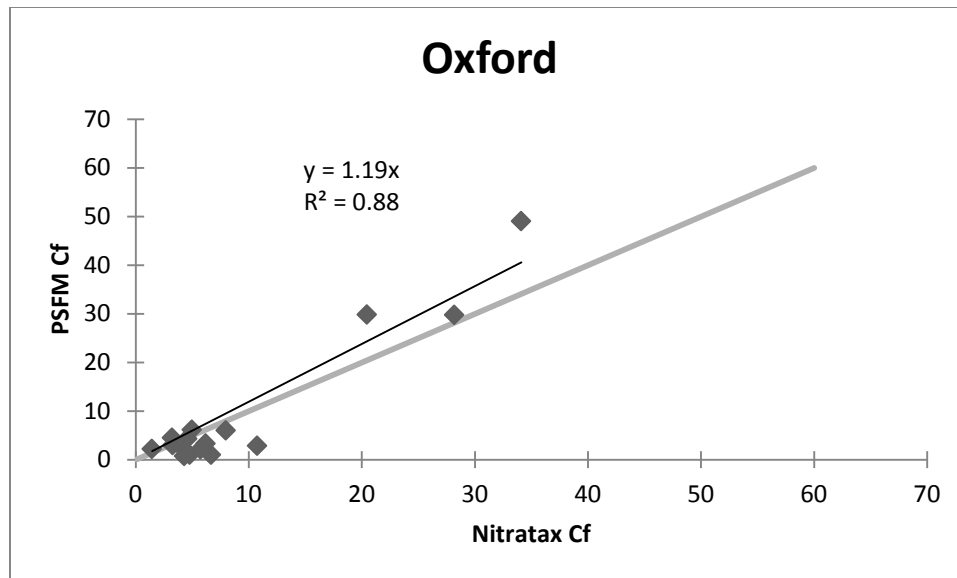


Figure 3.7 PSFM flow averaged concentration plotted versus Nitratax and USGS discharge flow averaged concentrations at the Oxford site.

Table 3.3 Flow-averaged concentrations of nitrate from PSFM and Nitratex for Coralville site.

Deployment Time	Collection Time	PSFM Mean Cf	PSFM Standard Deviation	Nitratex Cf
6/20/2012	6/27/2012	28.20	5.10	19.22
6/27/2012	7/5/2012	20.90	3.76	12.32
7/25/2012	8/1/2012	3.99	0.04	2.66
8/1/2012	8/8/2012	3.38	0.49	3.86
8/14/2012	8/22/2012	2.12	0.14	3.16
8/22/2012	8/28/2012			2.34
8/28/2012	9/5/2012	2.01	2.01	2.83
9/5/2012	9/12/2012	4.83	4.17	3.99
9/12/2012	9/19/2012	0.93	0.93	3.50
9/19/2012	9/26/2012			2.05
9/26/2012	10/3/2012			3.52
10/3/2012	10/10/2012	11.40	6.57	2.29
10/10/2012	10/17/2012	2.07	2.07	3.56
10/17/2012	10/24/2012			10.43
10/24/2012	10/31/2012	2.79	1.72	4.25
10/31/2012	11/7/2012			6.97

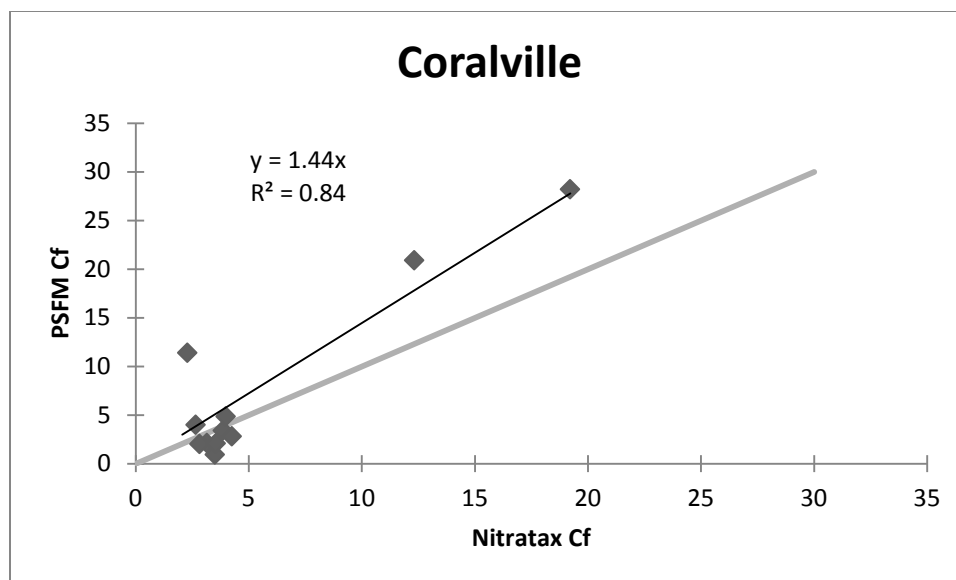


Figure 3.8 PSFM flow averaged concentration plotted versus Nitratax and USGS discharge flow averaged concentration at Coralville site.

### 3.4.2 Solute (Nitrate) Fluxes

Nitrate fluxes (kg/event) estimated by the PSFM (see Section 2.5.2 for methods) were compared with the fluxes measured by the Nitratax sensor. Results comparing the PSFM load with the Hach Nitratax load at the Oxford site can be seen in Figure 3.9. It can be seen that there is a strong linear regression with  $R^2$  of 0.98, though the PSFM is under estimating at this site by 27%. The results from the Coralville site, seen in Figure 3.10, are that the PSFM is under estimating by 34% but again there is a strong linear regression with  $R^2$  of 0.98. Combining all data points within Clear Creek, seen in Figure 3.11, the relationship between the PSFM and the Nitratax is that the PSFM is under estimating by 29% with a linear regression  $R^2$  of 0.98.

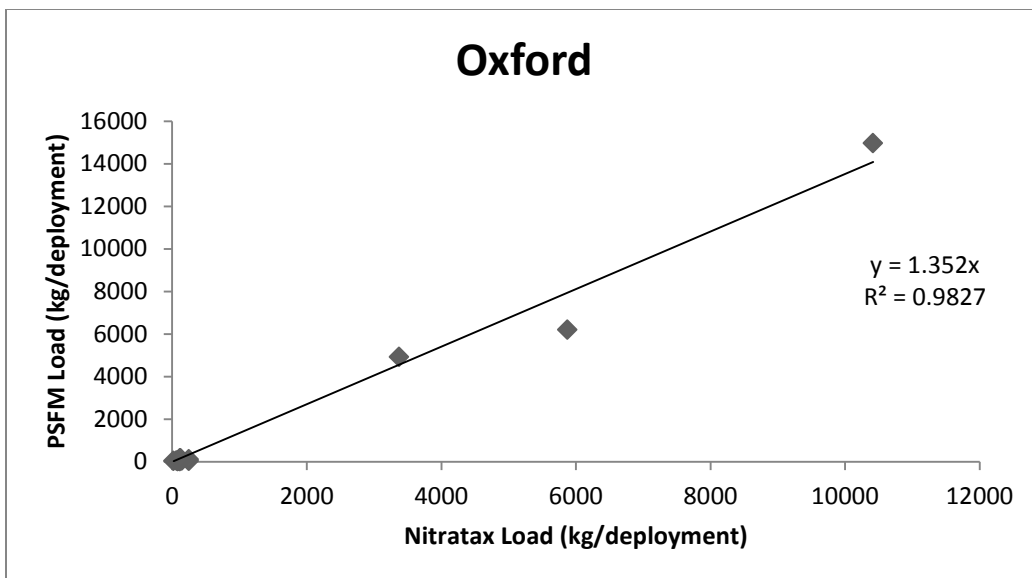


Figure 3.9 Nitrate load estimated by PSFM compared with nitrate load estimated from the Nitratex sensor data and discharge data from the Oxford site.

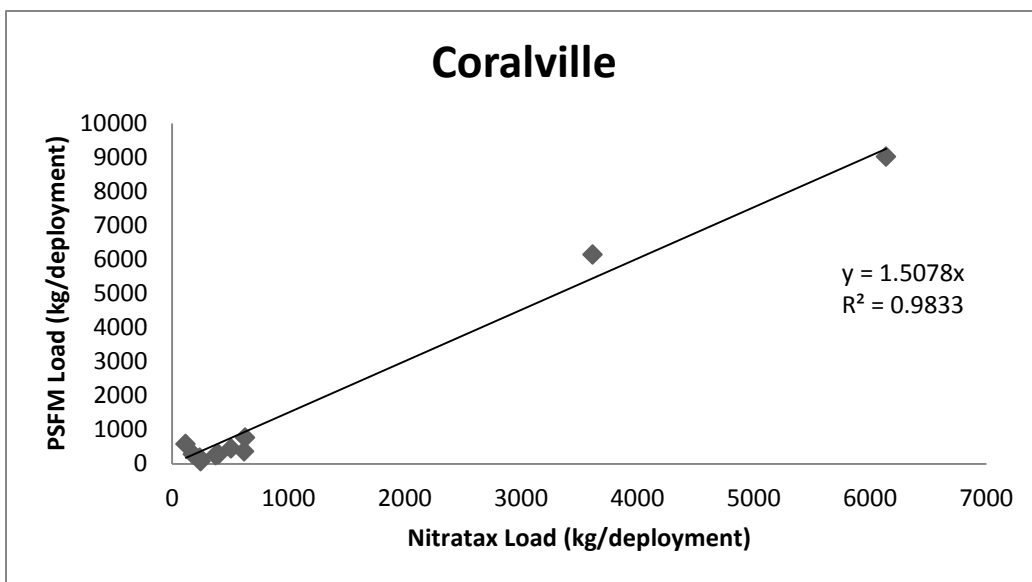


Figure 3.10 Nitrate load estimated by PSFM compared with estimated nitrate load from Nitratex and discharge data from the Coralville site.



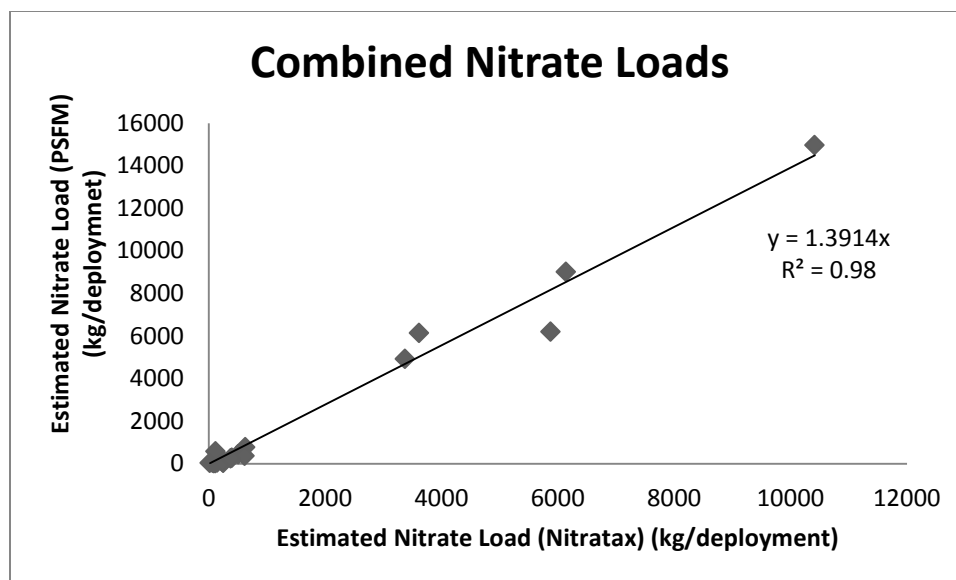


Figure 3.11 Nitrate load estimated by PSFM compared with estimated nitrate load from Nitratex and discharge data for both sites combined.

### 3.5 Discussion

There was a consistent linear relationship (correlation coefficients equal to 0.98) between the load estimated by the PSFM and that estimated by the Nitratex sensor over multiple storms within the 2012 season. The storm sizes per deployment varied over an order of magnitude from 0.17 to 9.58 mm at the Coralville site and 0.053 to 1.19 mm at the Oxford site, and the nutrient loads per deployment varied over two orders of magnitude between 115 to 10980 kg at the Coralville site and 21 to 10400 kg at the Oxford site. The consistency of the linear relationship between PSFM and Nitratex loads over such a range of storm sizes lends credence to the ability of the PSFM to estimate true loads under field scenarios.

The underestimation seen from the in-situ deployments was likely caused by the fact that the flow through the sampler is driven by a velocity gradient between the inlet and outlet that led to a pressure drop that varied non-linearly with the outside velocity, thus leading to a non-linear relationship between the inside and outside velocities, as discussed in equation 2.18. Such a non-linear relationship leads to a disproportionate weighting of the  $C_f$  estimate, and a corresponding

underestimate. Another possibility of the underestimation is microbial activity causing denitrification within the sampler over the deployment period. The ion exchange resin was not coated with any anti-microbial material therefore it is possible that the underestimation may be due to losses from denitrification. In order to eliminate this problem

### 3.6 Conclusion

Using the PSFM design by Boland (2011) a series of deployments within Clear Creek watershed were conducted. Results from the in-situ deployment were used to determine the relationship between PSFM load estimates and load estimates from a Nitratex probe and USGS discharge data. A consistent linear relationship was observed between PSFM and Nitratex loads over a range of storm sizes lends credence to the ability of the PSFM to estimate true loads under field scenarios. However, calibration would be required since the PSFM underestimated the true loads estimated by Nitratex by ~29%. This underestimation is most likely due to the non-linear relationship between stream velocity and velocity through the sampler. Another factor that could have contributed to error was a non-variable data set. Most data points taken over the summer were taken during very low flow events due to drought conditions. Therefore, a good estimate of the true relationship would require more data collected over a wider variety of deployment flow conditions. But using the data collected over the summer of 2012 there was an underestimation.

In order to overcome the underestimation of the PSFM in which flow through the sampler is dictated by the stream velocity, an alternate design was proposed in which the pressure difference driving the flow through the sampler is linearly proportional to the transient head above the sampler inlet. This design was created and tested in flume experiments of which the results can be seen in the following chapter.

## CHAPTER 4: ALTERNATE DESIGN OF PASSIVE SURFACE FLUX METER

### 4.1 Introduction

The field tests described in Chapter 3 indicated a linear relationship between estimated nutrient fluxes using the PSFM and the Nitratax sensor; however the PSFM underestimated the field fluxes. As described in previous chapters, this is attributed to the non-linear relationship between the velocity through the PSFM, and the velocity through the channel cross-section. To overcome this constraint, an alternate design of the sampler was conceptualized using pressure head to dictate flow through the sampler. Our objectives in this chapter are to: 1) describe design principles; 2) conduct flume experiments to test the design, and 3) develop field deployment parameters (sampler characteristics, duration of deployment, etc.) based on results from flume tests.

### 4.2 Device Theory and Construction

#### 4.2.1 Device Theory

The primary feature of the new design is that the flowrate through the PSFM varies linearly with the static head above the depth of deployment. The linear relationship between the flowrate through the PSFM and the pressure head at the deployment depth was achieved by connecting the outlet of the PSFM to a reservoir that is maintained at atmospheric pressure (Figure 4.1).

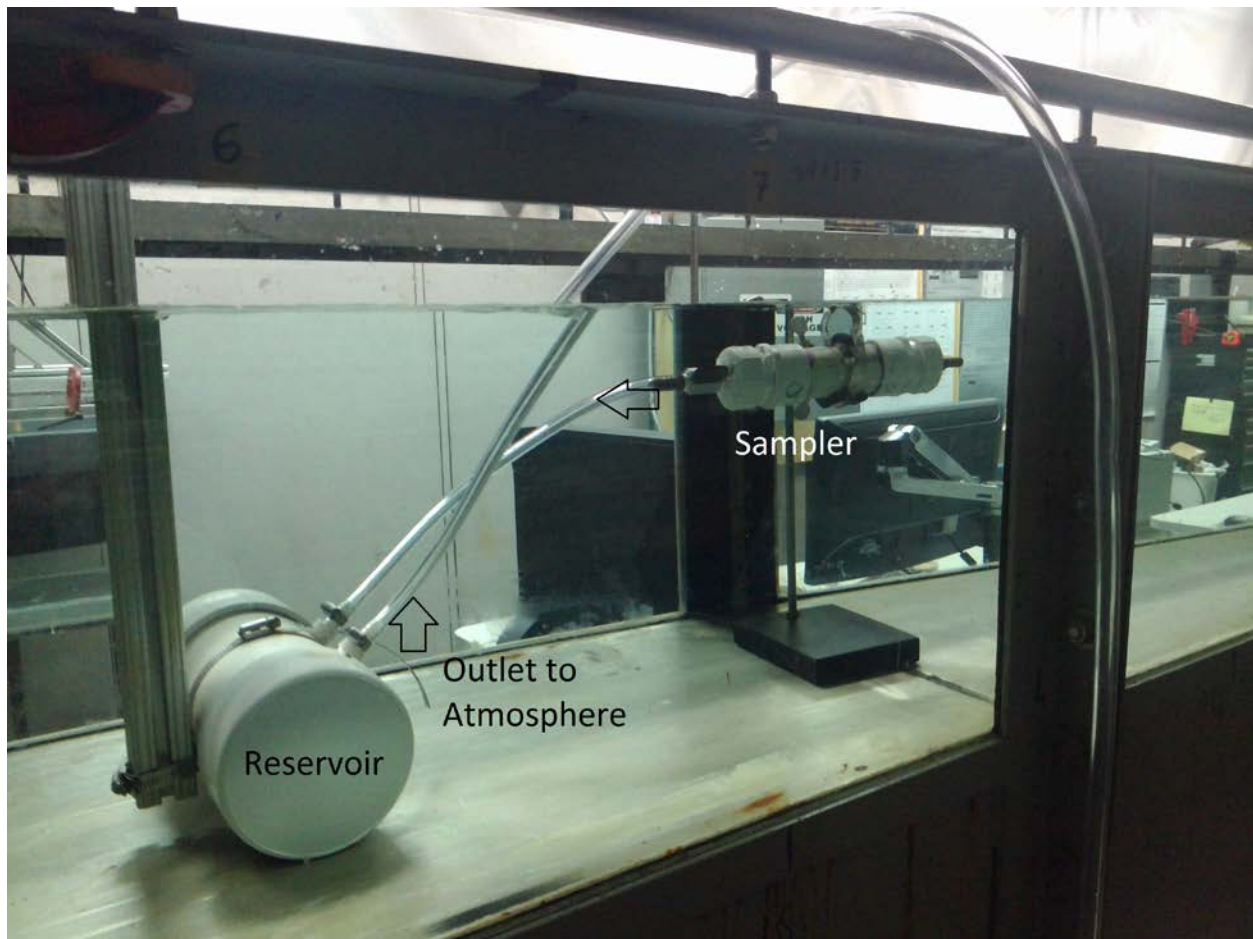


Figure 4.1 Experimental set up for flume experiments using the Reservoir PSFM. The reservoir is attached to a post to keep it from floating. The sampler was held at a constant depth using a clamp and ring stand.

Following Bernoulli's law, the headloss through the sampler is equal to the difference between the pressure head and velocity heads at the inlet and outlet, respectively.

$$\Delta H = \frac{1}{\rho g} (p_1 - p_2) - \frac{1}{2g} (v_2^2 - v_1^2) \quad (4.1)$$

During flume experiments the flume velocity was held constant at 0.4 m/s ( $v_1$ ) and with the reservoir configuration the outlet velocity can be assumed to be zero. Using equation 4.1 the difference between the velocity heads was determined to be 0.008 m. The pressure head dictated by the head of water above the inlet of the sampler was varied from 0.06 to 0.175 m and since

the outlet was maintained at atmospheric pressure these depth can be considered the pressure head. The difference in the pressure head is at least an order of magnitude higher than velocity head difference, and thus it can be assumed that the pressure head is dictating the flow through the device. In the next section, a series of flume experiments are described to test the linearity of the relationship.

#### 4.2.2 Device Construction

The required volume of the reservoir was determined to be equal to  $\sim 2L$ . The reservoir was constructed by cutting a 12" section from a 4" PVC pipe. Holes for the inlet and outlet were drilled and taped  $\sim 3$ " apart then  $3/8$ " thread/barb fittings were glued in the taps. Caps were then glued to each end of the PVC pipe being careful so no leaks were created. Two hose clamps were affixed to the body of the reservoir in order to secure it to a post below water. Hose clamps were used to secure  $3/8$ " tubing to each port, one was connected to the outlet of the sampler the other was allowed to be open to the atmosphere. The reservoir was affixed to a post just downstream of the samplers (Figure 4.1).

### 4.3 Laboratory Tests to Evaluate Reservoir PSFM Design

#### 4.3.1 Design of Flume Experiments

A re-circulating flume driven by a 7.5 horsepower Hupp Electric Motors pump controlled by a Magnetek GPD 505 variable frequency drive (VFD) was used. The flume has a test section that is 9.12 m long, with a total length including head and tail tanks of 11.42 m. The width of the flume is 0.61 m and the standard flow depth is 0.3 m. The VFD was set at a frequency 55 Hz for all runs and the depth was held constant at 0.36 m. The water in the flume was dosed with  $KNO_3$  and allowed to mix for 24 hours before starting the experiments to ensure that the aqueous  $NO_3^-$  is evenly distributed within the flume. The concentration of nitrate in the flume was measured before and after each deployment and varied between 7.82 and 11.5 mg/L as  $NO_3^-$ .

The objective of the flume tests was to evaluate whether the flow through the sampler was related linearly to the static pressure head above the deployment depth. To achieve this, five different deployment depths were selected 6.7, 8, 11, 13.5, and 17.5 cm. Three or more samples were tested in the flume at each depth for statistical assurance. The only exception was where only one sampler was placed at 0.06 m and two samplers at 0.067 m. A total of 19 samples were tested over 10 different runs. During each run two samplers were simultaneously placed in the flume. Samplers were placed 10 feet apart from each other so that the flow field at the inlet of each sampler was uniform while minimizing turbulence from the upstream sampler and reservoir. Deployment times in the flume were approximately one day, and the velocity in the flume was held constant at 0.4 m/s. The parameters for each test can be seen in Table 4.1.

Table 4.1 Summary of Flume Experiment Parameters

Head (m)	Velocity (m/s)	Overall Height of water column	Duration of Deployment (days)
0.06	0.4	0.36	1
0.067	0.4	0.36	1
0.067	0.4	0.36	1
0.08	0.4	0.36	1
0.08	0.4	0.36	1
0.08	0.4	0.36	1
0.08	0.4	0.36	0.99
0.11	0.4	0.36	1
0.11	0.4	0.36	1
0.11	0.4	0.36	1
0.11	0.4	0.36	1
0.11	0.4	0.36	1
0.11	0.4	0.36	1
0.135	0.4	0.36	1
0.135	0.4	0.36	1
0.135	0.4	0.36	1
0.135	0.4	0.36	1.01
0.175	0.4	0.36	0.9
0.175	0.4	0.36	0.9
0.175	0.4	0.36	1

#### 4.3.2 Sorbent Extraction and Analysis

Flowrate,  $Q_d$ , through the sampler was calculated using two different estimates. The first estimate was from the volume of water collected in the reservoir after a deployment that was divided by the deployment time to determine  $Q_d$ . The second estimate to determine  $Q_d$ , was by the use the alcohol tracers as defined by the methods in Chapter 2, in which the alcohols were extracted from ~1.5 g of GAC using 35 ml of Isobutyl alcohol. Because the deployments in the flume were only for ~1 day, only methanol and ethanol depletion were averaged to estimate  $Q_d$  through the device.

The mass flux of nitrate through the sampler was estimated based on the total mass of nitrate collected on the resin during the deployment period, and analyzed using the methods described in Chapter 2. The flux-averaged concentration of nitrate was estimated by dividing the mass flux  $M_d$  by the two estimates for water flux,  $Q_d$ .

#### 4.4 Results and Discussion

##### 4.4.1 Flow Velocity through the Reservoir PSFM

The  $Q_d$  through the device was determined using two different estimates as described in the previous section. The resulting  $Q_d$  for the estimates were plotted against the static pressure head at the sampler inlet in Figure 4.2 and Figure 4.3. A linear relationship was observed between the pressure head at the inlet, and the flow rate through the sampler, indicating that the design goal of linearity was achieved. Greater variability was observed for the alcohol tracer estimate, due to the inherent errors that can occur because of tracer volatilization and other losses during analysis. However, both methods yielded very similar slopes lending credence to the robustness of the design. The slope was used to estimate the effective hydraulic conductivity ( $K$ ) of the sampler following Darcy's Law. The estimated  $K$  using methods 1 and 2 were equal to 0.090 and 0.084 m/d, respectively. Due to inconsistency in packing outliers were tested using the statistical Q-test and those experiments that proved to be outliers were removed with 95% confidence.



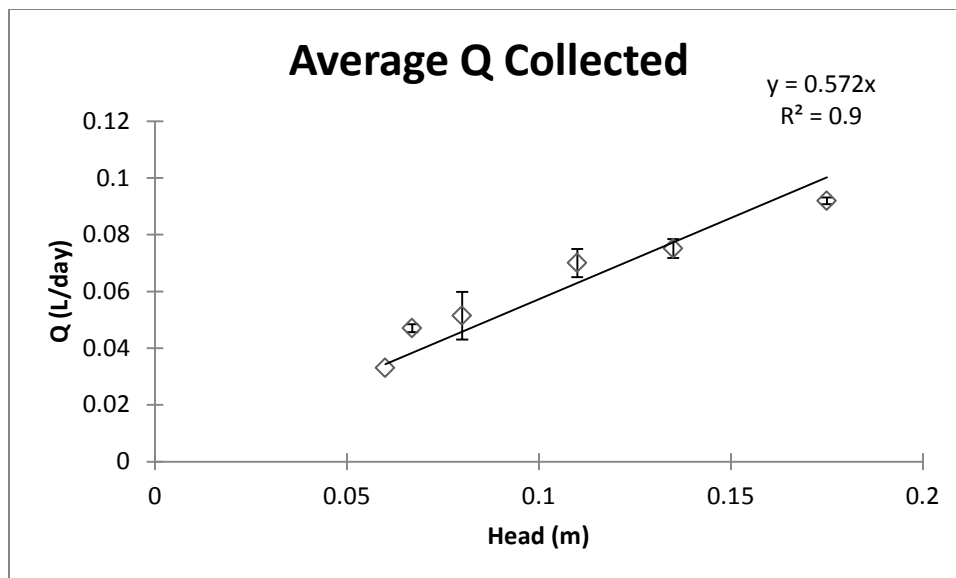


Figure 4.2 Average flowrate through the sampler plotted against the head driving the flow. Flowrate was calculated by the volume of water collected in the reservoir following each experiment.

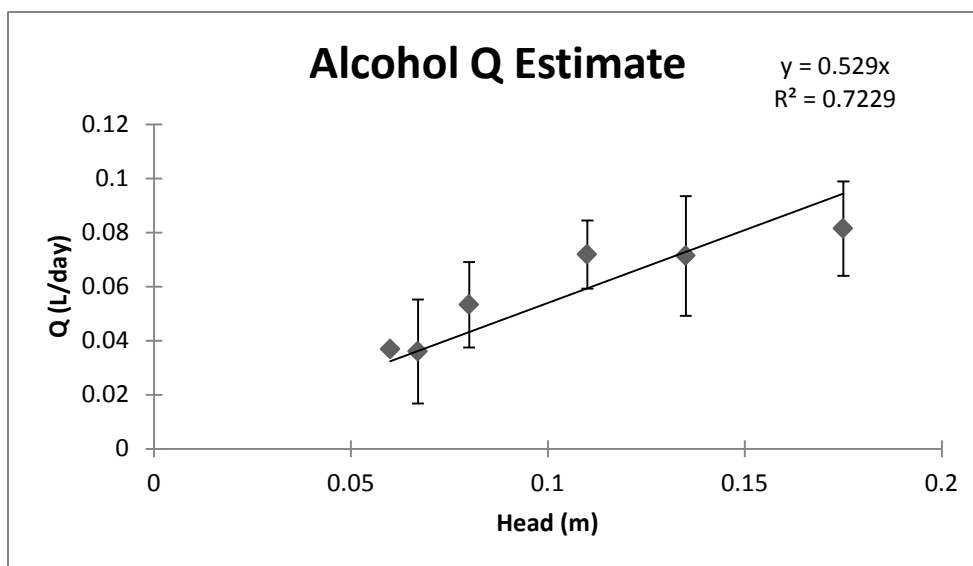


Figure 4.3 Average flowrate through the sampler plotted against the head driving the flow. Flowrate was estimated using the alcohol tracers.

#### 4.4.2 Nitrate Load and Flux-averaged Concentration Estimated by Reservoir PSFM

The flux-averaged concentrations of nitrate,  $C_f$ , estimated using the two  $Q_d$  values obtained in the previous section, were compared with the ambient concentration of nitrate in the flume. A one-to-one relationship should be seen as shown by the 45 degree line in Figure 4.4 and Figure 4.5. It can be seen that the Reservoir PSFM does a decent job of estimating the flux-averaged concentration of nitrate using both methods. There is some variability in the data but this could be caused by many sources of error in the experimental methods. Alcohols could be lost due to excessive exposure to air. The amount of initial interference on the resin could differ from sample to sample. Also high amounts of variability in the nitrate mass flux could also cause errors.

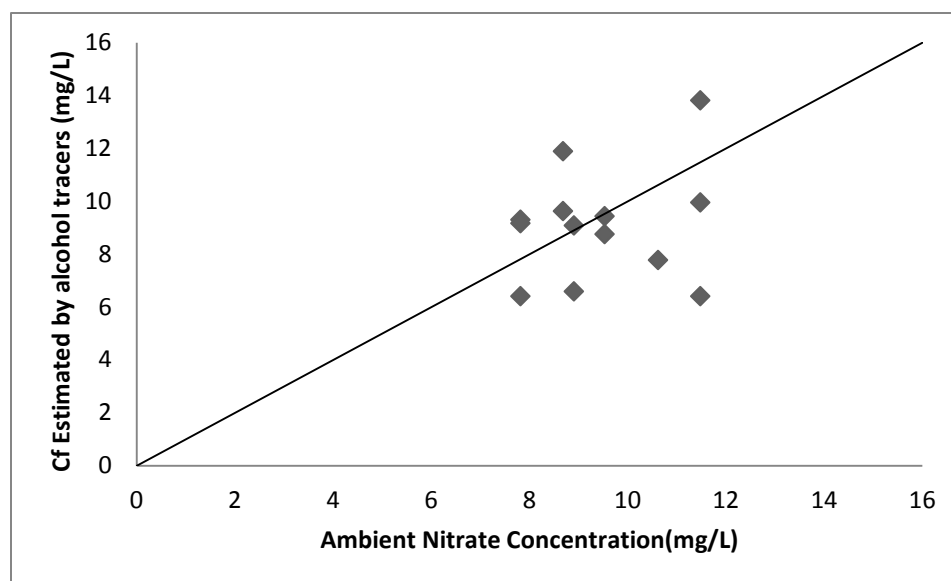


Figure 4.4 Flow-averaged concentration of nitrate estimated by alcohol tracers versus ambient concentration of nitrate in flume.

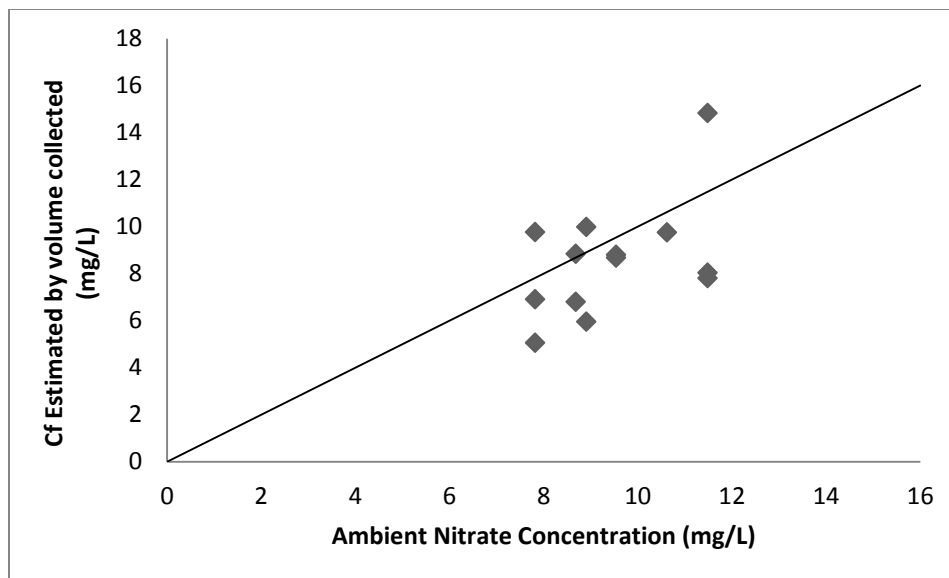


Figure 4.5 Flow-averaged concentration of nitrate estimated by volume collected versus ambient concentration of nitrate in flume.

#### 4.5 Design of Field Experiment

In order to estimate how the HD-PSFM would be deployed in the field, available data was used to create a framework for deployment techniques. First, two years of gage height data from the Oxford site was plotted in order to see variability in head over a deployment period (Figure 4.6). 22 storm events were isolated over the two year dataset (Table 4.2). Using the effective conductivity from the flume experiments the total flow through the Reservoir PSFM over the duration of these 22 storms were calculated. This was then plotted as a function of the size of the storms in Figure 4.7.

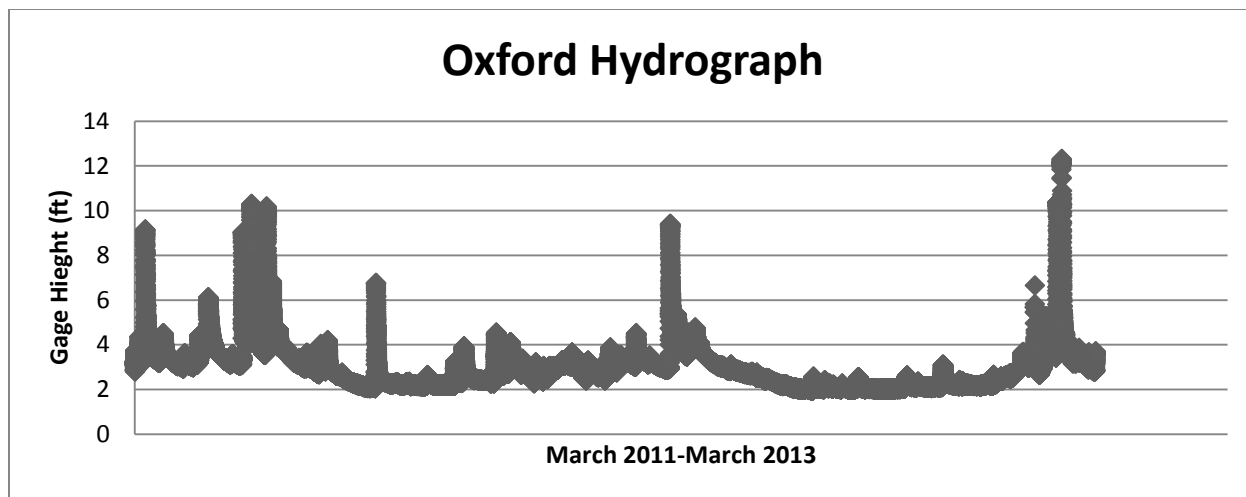


Figure 4.6 Hydrograph of USGS Oxford site.

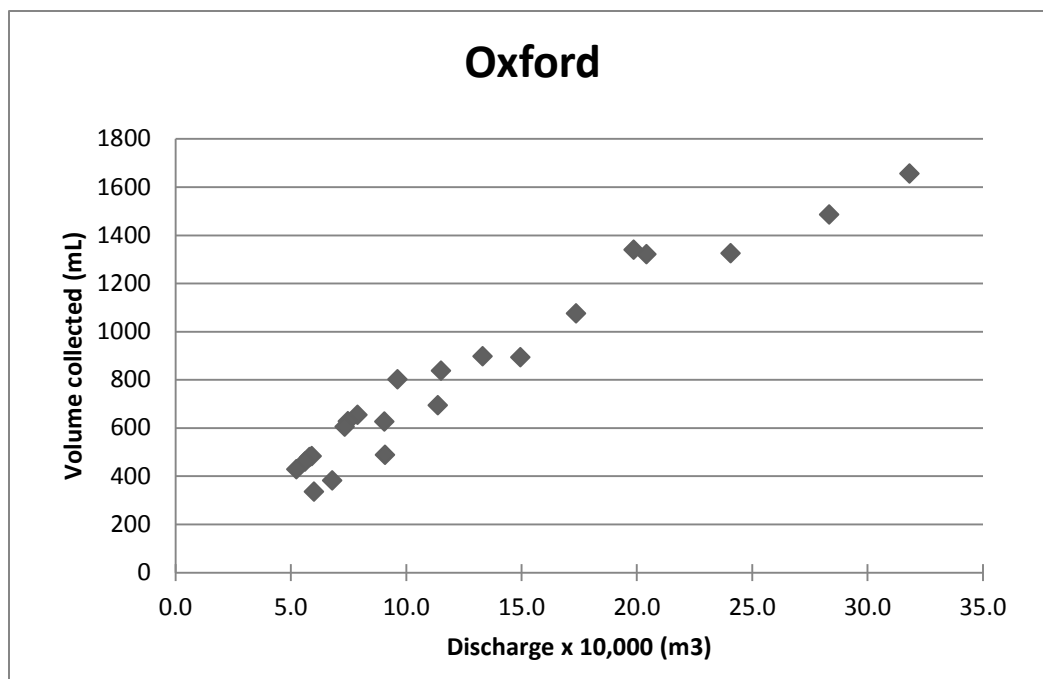


Figure 4.7 Distribution of 22 events during 2011 with a deployment depth of 2.5 ft from the streambed.

Table 4.2 Series of 22 events at the Oxford site using parameters from laboratory experiments to calculate total volume collected over the deployment time.

Event Size (mm)	Volume Collected (ml)	Event Time (Days)
0.52	654	7.00
1.35	1320	6.74
0.49	628	6.92
0.64	801	7.00
0.38	479	7.00
0.39	482	7.00
0.37	459	7.00
0.35	428	3.00
0.49	604	4.00
0.76	837	8.00
0.60	626	8.00
0.99	892	6.68
1.59	1325	3.92
1.87	1485	4.88
0.88	896	6.00
2.10	1655	5.08
1.15	1074	5.00
1.31	1339	10.00
0.75	693	10.00
0.60	488	10.00
0.40	334	6.00
0.45	381	7.00

Using Table 4.2 and Figure 4.7, the maximum volume of the reservoir required over the range of the storm events in 2011-2013 was 2 liters. Thus, the reservoir used in the current design is adequate.

Table 4.3 Omega values for alcohol after deployment.

Volume Collected (ml)	Event Time (Days)	$\omega$ Methanol	$\omega$ Ethanol	$\omega$ IPA	$\omega$ TBA
654	7.00	0	0	0.510	0.783
1320	6.74	0	0	0	0.544
628	6.92	0	0	0.524	0.789
801	7.00	0	0	0.400	0.734
479	7.00	0	0	0.641	0.841
482	7.00	0	0	0.639	0.840
459	7.00	0	0	0.656	0.847
428	3.00	0	0	0.250	0.668
604	4.00	0	0	0.207	0.649
837	8.00	0	0	0.451	0.757
626	8.00	0	0	0.589	0.818
892	6.68	0	0	0.298	0.689
1325	3.92	0	0	0	0.213
1485	4.88	0	0	0	0.291
896	6.00	0	0	0.216	0.652
1655	5.08	0	0	0	0.243
1074	5.00	0	0	0	0.500
1339	10.00	0	0	0.297	0.688
693	10.00	0	0	0.636	0.839
488	10.00	0	0	0.744	0.887
334	6.00	0	0	0.707	0.870
381	7.00	0	0	0.714	0.873

With this amount of flow going through the sampler the amount of alcohol remaining after deployment may be lower than the recommended  $C/C_0$  range of 0.200-0.850 as seen in Table 4.3. It can be seen that the short chain alcohols (Methanol, Ethanol) are completely depleted over the events, while the long chain alcohols (IPA, TBA) still remain for most small and medium size events. Ideally more than one alcohol should be used to estimate the flow

through the device. Thus modifications to the sampler would need to be made in order to determine an accurate flow average concentration in the field from the alcohol tracers.

Possible modifications that could be made to the sampler are to decrease the hydraulic conductivity by either increasing the length of sand layer or changing the sand particle size. Another media other than sand could also be used to decrease the hydraulic conductivity through the device as well. An alternative option would be to dose the GAC with alcohols having higher retardation coefficients thus allowing for longer deployments in the field. Also modifications to the way the sampler is deployed could be made. The sampler could be placed higher within the water column so that the static pressure head would not be as great during the full duration of a deployment but would only increase when a storm event takes place.

As stated previously ideally a researcher would be monitoring the flow through the device using a programed code which embodied the conductivity of the sampler, deployment depth, and gage height to determine when the sampler should be replaced so that accurate measurement of flow can be made and the alcohols will not be completely depleted from the GAC.

#### 4.6 Conclusion

Using the alternative static head driven PSFM design a linear relationship between flow through the device,  $Q_d$ , and the static head above the inlet should be observed. By connecting the outlet of the sampler to a reservoir held at atmospheric pressure and using Bernoulli's equation this design was mathematically conceptualized and a prototype was built. The prototype was then tested in a series of laboratory flume experiments at differing deployment depths to test the aforementioned theory.

Flow through the device was determined using two methods first the volume of water collected in the reservoir after deployment and second by using alcohol tracers. Both estimates provided similar results showing that  $Q_d$  is linearly proportional to the static pressure head above the sampler inlet. Using the plots from method 1 and 2, the effective hydraulic conductivity of

the alternative design was determined to be to 0.090 and 0.084 m/d, respectively. The effective hydraulic conductivity was then used in order to assess  $Q_d$  for field experiments, which was done for 22 events over a 2 year period at the Oxford site in Clear Creek. Results showed that a 2 liter reservoir would be adequate. Although these results also indicated that some changes would have to be made to the packing or deployment techniques so that the water flux could be estimated properly. Three alternatives were suggested including increasing of the hydraulic conductivity, the used of longer chain alcohols, and deployments at higher depths within the stream.



## CHAPTER 5: CONCLUSION

### 5.1 Motivation and Objectives

In order to keep our waterways fishable, swimmable, and drinkable in accordance with the CWA, assessment of TMDLs for impaired waterways must be made. TMDL's are assessed through the collection of data within the watershed. Data is often collected using either grab sampling or through the use of autosamplers or sondes. Using these techniques there are limitations including 1) the labor to collect samplers 2) only at a few points within the watershed can be monitored do to cost or time constraints and 3) data points must be linearly interpolated to integrate load in order to determine the TMDL for a given contaminant. Thus passive samplers have become a more relevant source for data collection, due to its ability to collect continuous time-averaged or flow-averaged nitrate loads within a watershed. Passive samplers are also a more cost effective way to characterize the spatial distribution of solute watersheds. Therefore, the development of a Passive Surface Water Flux Meter (PSFM) for spatially deployment in a watershed was investigated in this study. The objectives of the study were first to evaluate the ability of the PSFM developed by Boland (2011) to measure nitrate fluxes under transient flow conditions in a natural stream channel and second, to develop an alternate PSFM design based on lessons learned from the field study and test a prototype under laboratory conditions.

### 5.2 Results of In-situ Field Deployments

The PSFM design made by Boland (2011) was tested under transient flow in a stream channel at two locations within the Clear Creek Watershed. The PSFM estimated flow-averaged concentrations were compared with estimated based on USGS stream gage data for flow, and Nitratax data for concentration. A consistent linear relationship was apparent between the PSFM estimate and the Nitratax-USGS estimate. The consistency of the relationship over a range of flow events lends credence to the robustness of the device. While the relationship between the two estimates was linear, the PSFM consistently underestimated the Nitratax estimates by 36%. The underestimation implies that the PSFM needs to be calibrated against other methods of

measurement for the data to be reproducible. The underestimation is most likely due to the non-linear relationship between stream velocity and velocity through the sampler. This motivated me to think about an alternate design with linear relationship between the transient stream depth above the sampler and the flowrate through the sampler.

### 5.3 Results of Reservoir PSFM

Using the Reservoir PSFM a linear relationship between flow through the device,  $Q_d$ , and the static head above the inlet was observed. The prototype was tested in a series of laboratory flume experiments at differing deployment depths to test that flow through the sampler was linearly related to the static head above the inlet.

Flow through the device was determined using two methods 1) the volume of water collected in the reservoir after deployment and 2) alcohol tracers. Both estimates provided similar results showing that  $Q_d$  is linearly proportional to the static pressure head above the sampler inlet as theorized. The effective hydraulic conductivity of the alternative design was determined to be to 0.090 and 0.084 m/d, respectively using both methods. The effective hydraulic conductivity was then used to assess  $Q_d$  for field experiments. Results showed that a 2 liter reservoir would be adequate. Although these results also indicated that some changes would have to be made for proper assessment in the field. Three alternatives were suggested including increasing of the hydraulic conductivity, the used of longer chain alcohols, and deployments at higher depths within the stream.

### 5.4 Implications and Future Work

The PSFM is an inexpensive and versatile way to estimate total load within a stream. Because of its simple, inexpensive design the PSFM can be used for spatial characterization of contaminants within a watershed. As opposed to other sampling techniques, it can be placed at many different locations within a watershed for a fraction of the cost. Relationships between land cover and farming practice within the stream could then be assessed as well as testing to see if nutrient reduction techniques are working as theorized. Either the single chamber PSFM or the

Reservoir PSFM could be used for nutrient load assessments depending on the specification of the stream. The versatility of the design and packing of the sampler allow for applicability across a wide range of watershed and stream sizes.

In order to validate the Reservoir PSFM design field experiments would need to be conducted to show that the linear relationship seen in the flume experiments also applies to deployment in the field. Because only IPA and TBA would be remaining after a deployment of the Reservoir PSFM investigations into changing the packing of the sampler to decrease flow would also need to be investigated. Once these issues have been addressed the Reservoir PSFM could be spatially deployed within a watershed to better understand the correlation between land cover and nutrient loading. The initial field design could also be used knowing that a correction factor would have to be applied to the results in order to determine the correct nutrient load.

## BIBLIOGRAPHY

- 33 USC Section 1313. (n.d.). *Water quality standards and implementation plans*.
- Alewell, C., Lischeid, G., Hell, U., & Manderscheid, B. (2004). High temporal resolution of ion fluxes in semi-natural ecosystems - gain of information or waste of resources? *Biogeochemistry*, 69(1), 19-35.
- Boland, S. J. (2011). Hydrologic and Biogeochemical Signatures in intensively managed catchments: Data synthesis and development of a passive surfacewater quaily sampler. *Master Thesis, University of Iowa*.
- Cho, J., Annable, M. D., Jawitz, J. W., & Hatfield, K. (2007). Passive Flux Meter Measurement of Water and Nutrient Flux in Saturated Porous Media: Bench-Scale Laboratory Tests. *Journal of Environment Quality*, 36(5), 1266-1272.
- Cooter, W. (2004). Clean Water Act assessment processes in relation to changing U.S. Environmental Protection Agency management strategies. *Environmental Science and Technology*, 35(20), 5265-5273.
- De Jonge, H., & Rothenberg, G. (2005). New device and method for flux-proportional sampling of mobile solutes in soil and groundwater. *Environmental science & technology*, 39(1), 274-282. Retrieved from <http://www.ncbi.nlm.nih.gov/pubmed/15667105>
- Dean, K. (2011). Phosphorus Runoff to Clear Creek. *The University of Iowa, Master Thesis*.
- Diaz, R. J., & Rosenberg, R. (2008). Spreading dead zones and consequences for marine ecosystems. *Science*, 321, 926-929.
- Durhan, E. J., Lambright, C. S., Makynen, E. A., Lazorchak, J., Hartig, P. C., Wilson, V. S., . . . Ankley, G. T. (2006). Identification of metabolites of trenbolone acetate in androgenic runoff from a beef feedlot. *Environmental Health Perspectives*, 114, 65-68.
- Feng, Z., Schilling, K. E., & Chan, K.-S. (2012). Dynamic regression modeling of daily nitrate-nitrogen concentrations in a large agricultural watershed. *Environmental monitoring and assessment*. doi:10.1007/s10661-012-2891-7
- Fuortes, L., Clark, M. K., Kirchner, H. L., & Smith, E. M. (1997). Association between female infertility and agricultural work history. *American Journal of Industrial Medicine*, 31(4), 445-451.
- Gorecki, T., & Namies, J. (2002). Passive Sampling. *Trends in analytical chemistry*, 21(4), 276-291.
- Hatfield, K., Annable, M., Cho, J., Rao, P. S., & Klammler, H. (2004). A direct passive method for measuring water and contaminant fluxes in porous media. *Journal of contaminant hydrology*, 75(3-4), 155-181. doi:10.1016/j.jconhyd.2004.06.005

- Hatfield, K., Rao, P., Annable, M., & Campbell, T. (2002). Device and method for measuring fluid and solute fluxes in flow systems. *Patent US 6,402,547 B1*.
- Iowa Department of Agriculture and Land Stewardship, Iowa Department of Natural Resources, Iowa State University College of Agriculture and Life Science. (2012). *IOWA NUTRIENT REDUCTION STRATEGY: A science and technology-based framework to assess and reduce nutrients to Iowa waters and the Gulf of Mexico*.
- Kaneko, S., Inagaki, M., & Morishita, T. (2012). A simple method for the determination of nitrate in potassium chloride extracts from forest soils. *World Congress of Soil Science, Soil Solutions for a Changing World*, 4-7.
- Kemp, W. M., Testa, J. M., Conley, D. J., Gilbert, D., & Hagy, J. D. (2009). Temporal response of coastal hypoxia to nutrient loading and physical controls. *Biogeosciences*, 6, 2985-3008.
- King, K. W., & Harmel, R. D. (2003). Considerations in Selectiong a Water Quality Sampling Strategy. *American Society of Agricultural Engineers*, 46(1), 63-73.
- Klammler, H., Newman, M. A., Szilagyi, E., Padowski, J. C., Hatfield, K., Jawitz, J. W., & Annable, M. D. (2007). Initial Test Results for a Passive Surface Water Fluxmeter to Measure Cumulative Water and Solute Mass Fluxes. *Environmental Science & Technology*, 41(7), 2485-2490.
- Lanxess. (2006). PRODUCT INFORMATION LEWATIT® Mono Plus MP 500. Netherlands.
- Loperfido, J. V. (2009). High-frequency sensing of Clear Creek water quality : mechanisms of dissolved oxygen and turbidity dynamics , and nutrient transport. *PhD diss., University of Iowa*.
- Mayer, P., Tolls, J., Hermens, J. L., & Mackay, D. (2003). Equilibrium sampling devices. *Environmental Science & Technology*, 37(15), 270A-270A.
- Mississippi River Gulf of Mexico Watershed Nutrient Task Force. (2008). *Gulf Hypoxia Action Plan 2008*.
- Namieśnik, J., Zabiegała, B., Kot-Wasik, A., Partyka, M., & Wasik, A. (2005). Passive sampling and/or extraction techniques in environmental analysis: a review. *Analytical and bioanalytical chemistry*, 381(2), 279–301. doi:10.1007/s00216-004-2830-8
- Osterman, L. E., Poore, R. Z., Swazenski, P. W., Senn, D. B., & DiMarco, S. F. (2009). The 20th Century development and expansion of Louisiana hypoxia, Gulf of Mexico. *Geo-Mar Letters*, 29, 405-414.
- Padowski, J. C., Rothfus, E. A., Jawitz, J. W., Klammler, H., Hatfield, K., & Annable, M. D. (2009). Effect of Passive Surface Water Flux Meter Design on Water and Solute Mass Flux Estimates. *Journal of Hydrologic Engineering*.

- Papanicolaou, A. N., Elhakeem, M., Wilson, C., Burras, C. L., & Oneal, B. (2008). Observations of Soils at the Hillslope Scale in the Clear Creek Watershed in Iowa , USA. *Soil Surv. Horiz.*, 49, 83-86.
- Putney, M. K. (2010). Using high frequency data collection to study nitrate on clear creek during flow events. *Masters Thesis, University of Iowa.*
- Rabalais, N. N., Turner, R. E., & Wiseman, W. J. (2002). Gulf of Mexico hypoxia, aka "The Dead zone". *Annual Review of Ecology and Systematics*, 33, 235-263.
- Rabalais, N. N., Wiseman, W. J., Turner, R. E., SenGupta, B. K., & Dortch, Q. (1996). Nutrient changes in the Mississippi River and system responses on the adjacent continental shelf. *Estuaries*, 19(2B), 386-407.
- Rayburn, A. P. (2006). Using the past to plan the future: Retrospective assessment of landscape and land-use change in the Clear Creek watershed, Iowa. *University of Iowa, Masters Thesis.*
- Rozemeijer, J., Van der Velde, Y. P., De Jonge, H., Van Geer, F., Broers, H.-P., & Bierkens, M. (2010). Application and evaluation of a new passive sampler for measuring average solute concentrations in a catchment scale water quality monitoring study. *Environmental Science and Technology*, 44(4), 1353-1359.
- Seethapathy, S., Górecki, T., & Li, X. (2008). Passive sampling in environmental analysis. *Journal of chromatography*, 1184(1-2), 234-253. doi:10.1016/j.chroma.2007.07.070
- Smith, V. H., Tilman, G. D., & Nekola, J. C. (1999). Eutrophication: impacts of excess nutrient inputs on freshwater, marine, and terrestrial ecosystems. *Environmental Pollution*, 100(1-3), 179-196.
- Soto, A. M., Calabro, J. M., Precht, N. V., Yau, A. Y., Orlando, E. F., Daxenberger, A., . . . Sonnenschein, C. (2004). Androgenic and estrogenic activity in water bodies receiving cattle feedlot effluent in eastern Nebraska, USA. *Environmental Health Perspectives*, 112(3), 346-352.
- Stone, M., & Krishnappan, B. (1997). Transport characteristics of tile-drain sediments from an agricultural watershed. *Water Air Soil Pollution*, 99((1-4)), 89-103.
- Tilman, D. (1999). Colloquium Paper: Global environmental impacts of agricultural expansion: The need for sustainable and efficient practices. *Proceedings of the National Academy of Science*, 96(11), 5995-6000.
- Vrana, B., Allan, I. J., Greenwood, R., Mills, G. A., Dominiak, E., Svensson, K., . . . al., e. (2005). Passive sampling techniques for monitoring pollutants in water. *Trends in Analytical Chemistry*, 24(10), 845-868. doi:10.1016/j.trac.2005.06
- Winchester, P. D., Huskins, J., & Ying, J. (2009). Agrichemicals in surface water and birth defects in the United States. *Acta Paediatrica*, 98(4), 664-669.

Zabiegała, B., Kot-Wasik, A., Urbanowicz, M., & Namieśnik, J. (2010). Passive sampling as a tool for obtaining reliable analytical information in environmental quality monitoring. *Analytical and bioanalytical chemistry*, 396(1), 273-296. doi:10.1007/s00216-